“A global lake and reservoir volume analysis using a surface water dataset and satellite altimetry” by Busker et al.

Cover letter to the editor

08 August 2018

Dear Prof. Anas Ghadouani,

I am pleased to submit the revision report of our paper “A global lake and reservoir volume analysis using a surface water dataset and satellite altimetry” (hess-2018-21).

We really appreciated all three referee comments and we have addressed them during the open discussion. A point-wise overview of these comments and suggestions with our responses and proposed corrections is attached below. Subsequently, a marked-up manuscript version is provided. Please note that revised figures appear on top of their older version.

We hope that this version is now acceptable for publication in the journal and that it may contribute to monitoring techniques of lakes and reservoirs from space.

With kind regards,

Tim Busker

Response to RC1 by Anonymous Referee #1

This paper explores the use of the JRC global surface water dataset, and the DAHITI satellite altimetry database to estimate hypsometry relationships for a reasonable number of lakes across the globe. The paper should be of interest to a people working in water resources, and potentially is a publishable paper.

Thank you a lot for your time, effort and useful feedback. We agree that our work should be of interest to many people working in water resources and hydrological modelling, as it improves on monitoring techniques of lakes and reservoirs currently available.

At the moment however, the paper is a fairly simple data analysis with insufficient statistics (i.e. uncertainties) warrant publications as it is. Might improve the paper if the authors consider what they learnt from analysing the dataset, and what limits would they place on the size of the dam might suit using this approach, rather than given vague qualitative statements. While the paper appears to be overall well written, there are some issues with the material presented (see comments below), and it would be good to have estimates of the uncertainty in the regressed coefficients (maybe indicated through confidence bounds on the fitted functions shown in the plots would be best?). I think the paper needs some revision before being ready for publication.

We agree that we can improve on these factors, especially on the uncertainty analysis, the application of the dataset and the limitations of satellite altimetry. In the comments below, we try to clarify on these points by either improving current explanations or by extending the analysis. We propose to include these revisions in the revised paper. Also, we found a data gap in the Tibetan Plateau, so we would like to fill this gap by analysing five additional lakes in this region.

Specific comments

1) Page 1, lines 19-25: the average r is given across 18 lakes. Would be good to know what the standard deviation is also as this would at least give the reader some idea of the scatter.

Proposed correction: We will include the standard deviation of the R^2 of the regression and of the Pearson correlation coefficient r in the abstract.

2) Page 4, lines 25-28: The definition of a large lake (ocean-like conditions) is a little vague. Might be useful to have a quantitative definition of what a large lake and a small lake are? Maybe something related to the minimum width of the widest part of the lake?

It would have been better to provide a quantitative definition of a large lake and a small lake here, to be clear about which lake sizes are expected to give a certain altimetry accuracy. If the altimetry accuracy was directly related to lake size, we could have been more explicit about the 'large and small' terms in this paragraph. This is however not the case. Large lakes are more likely to give a higher accuracy than smaller lakes, but we found no direct clear relationship between lake size and accuracy. Altimetry accuracy is dependent upon many other factors, like surrounding topography, surface waves, the shape of the water body, the sensor, and the position of altimeter track crossings. However, we mention the minimum lake size of a few hundred meters that can still yield accurate altimetry measurements, only in case all above mentioned conditions are ideal.

Proposed correction: Although we cannot be much more explicit in the term 'large and small' lakes, we totally revised section 2.1 to expand our explanation on the different causes of altimetry uncertainty and the complications for small water bodies.

Revised text for the second paragraph of section 2.1 (starting on line 5, page 4): 'The estimation of water level time series for small lakes, reservoirs or rivers is very challenging. Due to coarse mission-dependent ground tracks with a cross-track spacing of a few hundred kilometres, larger lakes and reservoirs have a much higher probability to be crossed by a satellite track than smaller ones. Moreover, small water bodies tend to have a relatively big altimeter footprint compared to their size, which will affect the resulting shape of the returning waveform. The diameter of the footprint is mainly influenced by the water roughness (i.e. surface waves) and surrounding topography. In reality, the diameter of the footprint can therefore vary between 2 km over the ocean and up to 16 km for small lakes with considerable surrounding terrain topography (Fu and Cazenave, 2001). These land influences and surface waves within the altimeter footprint can affect the altimeter waveforms and require an additional retracking to achieve more accurate ranges. In order to achieve accurate results for small water bodies, the conditions have to be ideal, meaning a low surrounding topography, low surface waves and perpendicular crossings of the altimeter track and the water bodies shore. In these ideal cases, satellite altimetry has the capability to observe rivers with a width of about 100-200 m or lakes with a diameter of a few hundred meters. The off-nadir effect is another problem which can occur when investigating smaller water bodies. In general, satellite altimetry measures in the nadir direction, but if the investigated water body is not located in the center of the footprint, then the radar pulses are not reflected in the nadir direction which leads to longer corrupted ranges that must be taken into account (Boergens et al., 2016)'.

Revised text for fourth paragraph of section 2.1 (starting on line 25, page 4): 'The quality of the water level time series from satellite altimetry in DAHITI has been validated with in-situ data. For large lakes with ocean-like conditions (such as the Great Lakes), accurate measurements can potentially be achieved with a root-mean square error (RMSE) as low as 4-5 cm, while for smaller lakes and rivers the RMSE could increase towards several decimeters (Schwatke et al., 2015a). However, no clear relationship was observed between lake size and altimetry accuracy, as the quality of water level time series is not only dependent on the target size, but also on many other factors (e.g. surrounding topography, surface waves, winter ice coverage, the position of altimeter track crossings).'

3) Page 10, Figure 4: there are large departures in the plot for Lake Nasser – what could cause these? How significant are they?

These outliers may be caused by time lags between altimetry measurements and Landsat observations in the GSW dataset, as explained in the second paragraph of section 5.3. We cannot correct for this uncertainty, as the GSW dataset did not save the exact dates of the Landsat observations, but only provides the month of observation. Therefore, the time lag between the measurements can be up to one month. In this extreme case of the outliers for Lake Nasser, both water levels were measured in the beginning of the month (2th and 6th day) and were the only measurements available during that month. For the next month, we observed a considerable change in water level. The area and water level observations thus likely referred to different lake conditions, which could be a reasonable cause for the outliers seen in Figure 4d in the manuscript. However, these specific outliers do not have a large influence on the regression as they represent only 5 % of the residuals (n=41). Considerable outliers caused by this effect are rare, as the water level change within a month has to be big, the number of altimetry measurements limited and the difference in timing of the A and h observations considerable. However, we expect this effect to be an important overall contributor to the residuals. To account for the area-level regression uncertainties, we extend the analysis by estimating residual-based confidence intervals (see comment 7).

We will add the following sentences to the revised version of the paper (page 19, line 8): 'The outliers in the regression of Lake Nasser (Figure 4d) are expected to be largely induced by this uncertainty. For both outliers, the altimeter measurements were taken in the beginning of the month (2th and 6th day), and the water level changed considerably towards the next month. The Landsat observation therefore likely measured different lake conditions than the satellite altimeter'.

4) Page 11, lines 14: It would be good to give some information on how the uncertainty was obtained, and how the no data pixels were treated in estimating the points shown in Figure 6. Are the red points likely to be lower bounds on the lake volume? From the Figure, these seems to be the case. If they are lower bounds, then the red shaded area seems to span between this low bound and an estimated upper bound. How are the individual pixels within the MWE converted to an area?

Is this simply adding up the number of pixels with a detection of a water surface? Appears to be so based on what I can see, in which case this is a very simplified approach, and better estimates of the upper and lower bounds could be made by considering the part of wet pixels at other times (I note that some discussion on this appears in page 18, reinforcing my interpretation that the simplified approach has been used).

The uncertainty described here is the uncertainty directly induced by the no data pixels within the maximum water extent (MWE). As described on page 7, line 25, the no data fraction (no data pixels within the MWE / all MWE pixels) was limited to only 5 %. These no data pixels are located within the MWE, and have thus been classified as surface water at least once over 1984-2015. This means there is a probability that they are water for that specific month. Therefore, the area of these no data pixels is simply added to the observed monthly lake areas, and the upper limit of the volume estimate is subsequently calculated using this upper area limit. To conclude, the red and blue lines in the volume variation plots (figure 6 in the manuscript) are our best volume estimates calculated with observed water area values. If any of the no data pixels within the MWE were covered by water, the estimated volume variation will be somewhere in the red shaded area.

This is indeed a simplified approach, but at least gives an indication of the amount of 'no data' and how this can affect the volume estimations. Techniques that can improve on this limitation are outlined in lines 12-18, page 18, and they got potential for further research. However, for this research we chose to use only direct observations of surface water, as these techniques to reduce 'no data' induce additional uncertainties and their complexity requires a whole new study.

However, we agree that we can explain this uncertainty in more detail. **Therefore we propose to substitute the sentence in line 13-16, page 11** with: 'The red line displays the best estimate of the volume variation as calculated with observed water classifications in the GSW dataset (i.e. total area of surface water). The red shaded area displays the upper volume boundary on the V_{GSW} estimates, as derived from the GSW dataset pixels classified as no data within the MWE (max 5 %, see section 3.2). These no data pixels could theoretically be covered with water for that month, and this would increase the estimated area. In this case the volume variation estimation would be somewhere within the red shaded area. The upper limit of the red shaded area would thus be reached if all no data pixels within the MWE contain surface water during that particular month.'

5) Page 14, lines 8-13: Information on data sources seems to be incomplete. Sources for US, Spain and Sudan are given, what about the source for the 2 lakes in Australia?

You are right, we forgot to mention the source of the 2 lakes in Australia. We will add the link in the revised manuscript. **We will add the following sentence to the revised version of the paper (page 14, line 13)**: 'Validation data for Lake Argyle and Lake Eucumbene were obtained from WaterNSW in Australia via http://realtimedata.water.nsw.gov.au/water.stm.'

6) Page 14, lines 13-14: Seems strange to make the statement that the NRMSE is relatively low taking into account all sources of uncertainty, but there is no discussion about what the sources of uncertainty are that have been considered, or the magnitude of the overall uncertainty. Does this statement mean that the NRMSE is a lot smaller than would be expected given the estimated uncertainty? If so, it suggests a possible error in the uncertainty quantification (e.g. ignoring the impact of serial correlation between the different component uncertainties).

We fully agree with you, so this sentence should be deleted. This statement is uninformative, as we do not quantify the total uncertainty as induced by all different uncertainties mentioned in the discussion.

7) Page 15, line 1: Yes, extrapolating beyond the limits of the data will result in higher errors. This is why the uncertainty in the regressed coefficients should be reported. Even then, the uncertainty estimated from the regressed quantities will be a lower bound on the uncertainty in the extrapolation as the estimate is based on the assumption that the fitted function still holds. Possible explanation for the over-estimation of the extrapolated storage for Lake Mead shown in Figure 8 (regressed coefficients are time dependent, or relationship is not as linear as was originally thought), or is the red line shown there within the uncertainty bounds for the original regression?

We agree that including the regression-based uncertainty may provide useful information for understanding estimation errors. Therefore, we estimated the regression uncertainty based on the standard deviation of the residuals, assuming they have a zero-mean Gaussian distribution $\varepsilon \sim N(0, {\sigma_\varepsilon}^2)$. From this residual-based uncertainty, we derived confidence intervals (CI) around the volume variation estimates.

Proposed correction: In the revised manuscript we will substitute the residual term ε_i with the $\frac{1+\alpha}{2}$ and $\frac{1-\alpha}{2}$ quantiles of the Gaussian distribution of ε to estimate a 95 % CI around the regression (see Figure 1).

We revised the old volume plots without a CI (Figure 6 in the manuscript) to volume plots with the 95 % residual-based CI (Figure 2) and the old validation plots (Figure 9 and 10 in the manuscript) to validation plots including the CI (Figure 3 and 4).

This CI represents the uncertainty directly from the standard deviation of the residuals. This is a lower limit of the actual uncertainty, as it does not account for model uncertainty (i.e. it assumes that the fitted linear function holds). However, still an average of 60 - 65 % of the validation volume variations fall inside the 95 % CI for the 18 validation lakes. This suggests that the majority of the uncertainty is captured.

Equation (2) and (3) now estimate the expected value of the volume $E[V_i]$. **After these equations, on line 24, page 7, we will add the following**:

'Subsequently, a confidence interval (CI) was calculated around the expected value of the volumes calculated with A. The residual term in Eq. (1) was included in the volume calculation (Eq. 3) to estimate the residual uncertainty on the expected volumes calculated with A values. It is assumed that the residuals have a zero-mean Gaussian distribution $\varepsilon \sim N(0, {\sigma_\varepsilon}^2)$, where σ_ε is the standard deviation of ε. To obtain the α-probability CI around the expected volume $E[V_i]$, the residual term is replaced by its $\frac{1+\alpha}{2}$ and $\frac{1-\alpha}{2}$ quantiles:

$$CI_{E[V_i]} = \frac{a \cdot {A_i}^2}{2} \pm \frac{A_i}{2} \cdot \sigma_\varepsilon \cdot \Phi^{-1}\left(\frac{1+\alpha}{2}\right)$$

Where $\Phi^{-1}\left(\frac{1+\alpha}{2}\right)$ is the inverse of the cumulative density function of the standardized Gaussian distribution (mean = 0, standard deviation = 1) at probability level $\frac{1+\alpha}{2}$. In this research, a 95 % CI has been used.'

It should be noted that the CI for the altimetry volume estimates is not shown in the plots, to keep them readable. They could be simply derived using the same methodology (i.e. by expressing the volume in terms of water level instead of area).

Additional remark for Lake Mead: For the extrapolated part of the volume variations we are not sure about the bathymetry of the lake, as we do not know if the estimated bathymetry in the regression will hold for extreme h or A values that are outside the h-A domain of the regression. For Lake Mead, this uncertainty likely caused the overestimation of the volume variation since 1984. This could mean that for the extrapolated part of the regression, the change in water level is in reality less sensitive to a change in lake area than what would have been expected given the found hypsometry (i.e. the slope of the regression is in reality less steep). If the water levels for the whole range of A values were included, the regression would therefore most likely either be explained by (1) a linear regression with a more gentle slope or (2) a regression with decreasing slope for higher A values. However, by comparing the in situ volume variations with the satellite estimations (Figure 8 of the manuscript), we hypothesize that a linear regression would still hold, but with a more gentle slope. This would probably avoid the overestimation as is observed for the extrapolated volumes now.

8) Page 19, lines 2-5: A non-linear hypsometry relationship shouldn't mean the lake volumes are unreliable. Just that more care and some more maths is needed to derive the volumes. The main issue would be the choice of fitted function, and how

this behaves under extrapolation. Given the result shown in Figure 12, a hyperbolic function that becomes roughly constant as area decreases and linear as area increases would likely be a much better function to fit than a quadratic or a cubic.

I think there is a misunderstanding about this sentence as we did not clearly formulate it. We do not suggest that volumes of these non-linear lakes are unreliable, but that for these lakes the volumes estimates assuming linear area-level relations are unreliable. So with our current methodology, the calculated volumes are assumed to be unreliable for these lakes.

Proposed correction, **page 19, line 2-3**: 'Only three out of 135 lakes (Tawakoni, Urmia and Eagle) showed a clear non-linear area-level relation. For these lakes, volume variations were not estimated'

Minor comments

1. Page 5, line 26 (and elsewhere): might be better to have all acronyms in capital letters.

Yes thank you, we will check all acronyms and revise this.

2. Page 9, line 11: "Lakes Powell, Kariba, Mead and Nasser"

This will be corrected in our revised document.

3. Page 12, line 6 (and elsewhere): km3 is not a standard SI unit. The equivalent SI unit would be TL (teralitres). Is km^3 acceptable?

Yes this is a HESS guideline, as indicated in the 'Manuscript preparation guidelines for authors'.

4. Page 12, line 23: "during which time it lost approximately 30 km3"?

Yes, this is a better formulation. We will revise this in our manuscript.

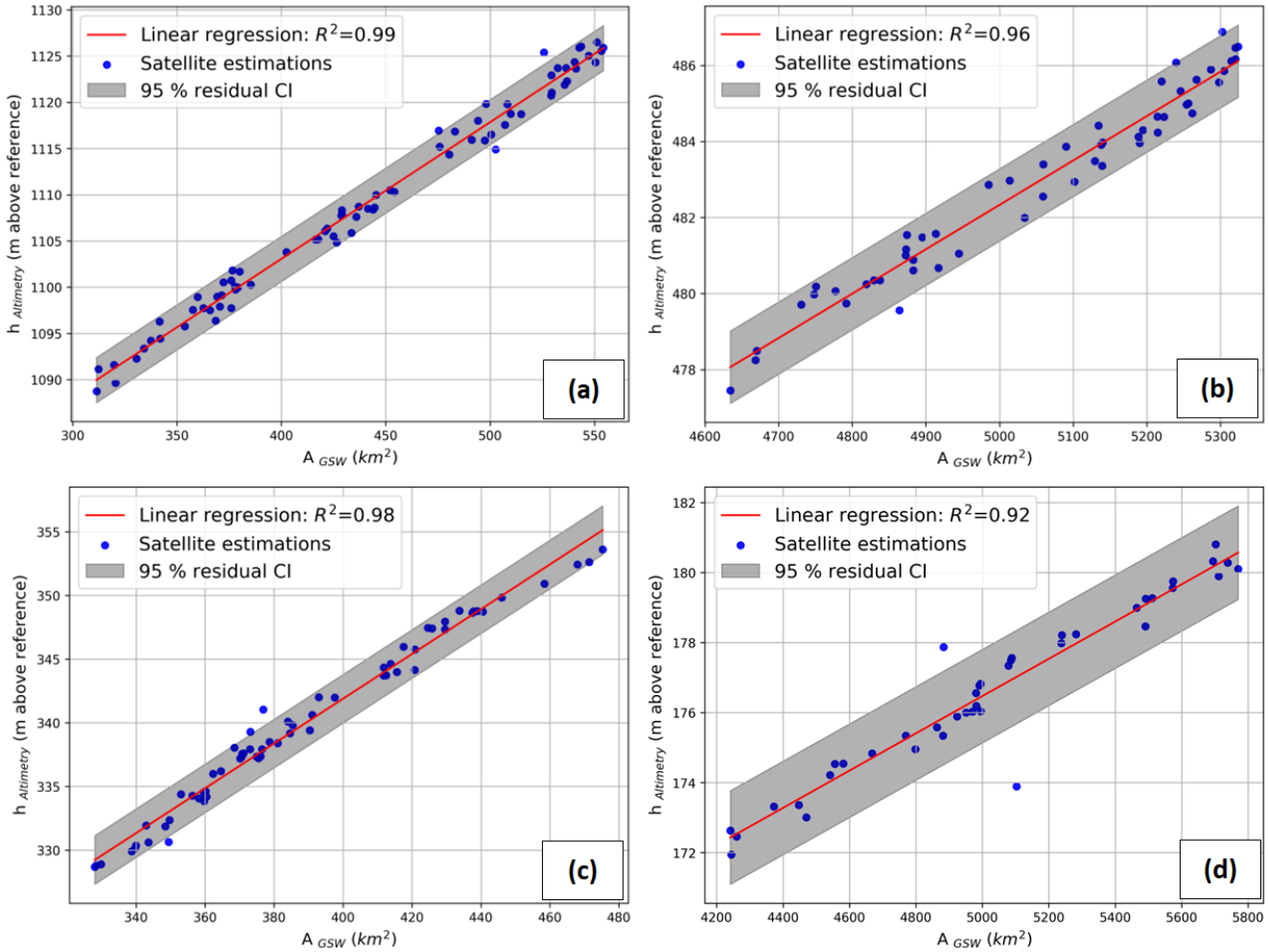

Fig. 1 Area-level regressions for Lake Powell (a), Kariba (b), Mead (c) and Nasser (d), with R2 values of respectively 0.99, 0.96, 0.98 and 0.92.

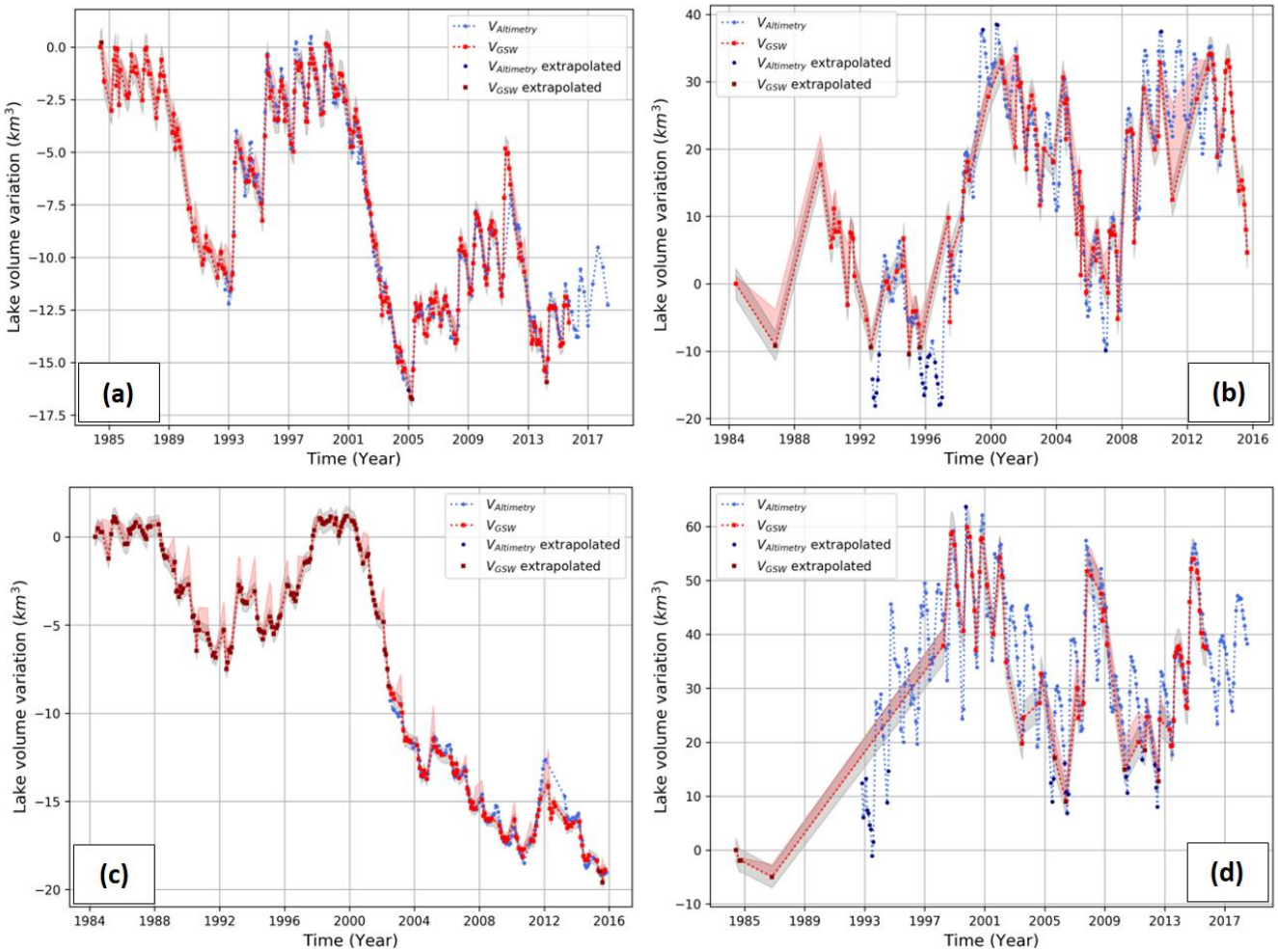

Fig. 2 Lake volume variations for Lake Powell (a), Kariba (b), Mead (c) and Nasser (d) using $V_{Altimetry}$ (blue) and V_{GSW} (red).

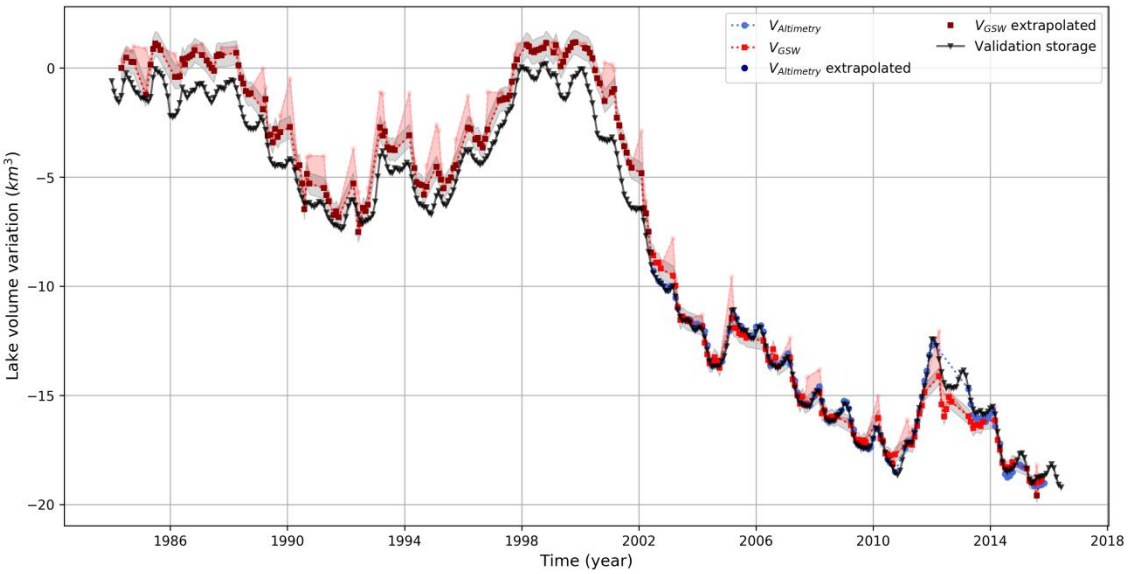

Fig. 3. Validation time series plotted with estimated reservoir volumes for Lake Mead. The black triangle line represents the validation storage as measured using the full lake bathymetry.

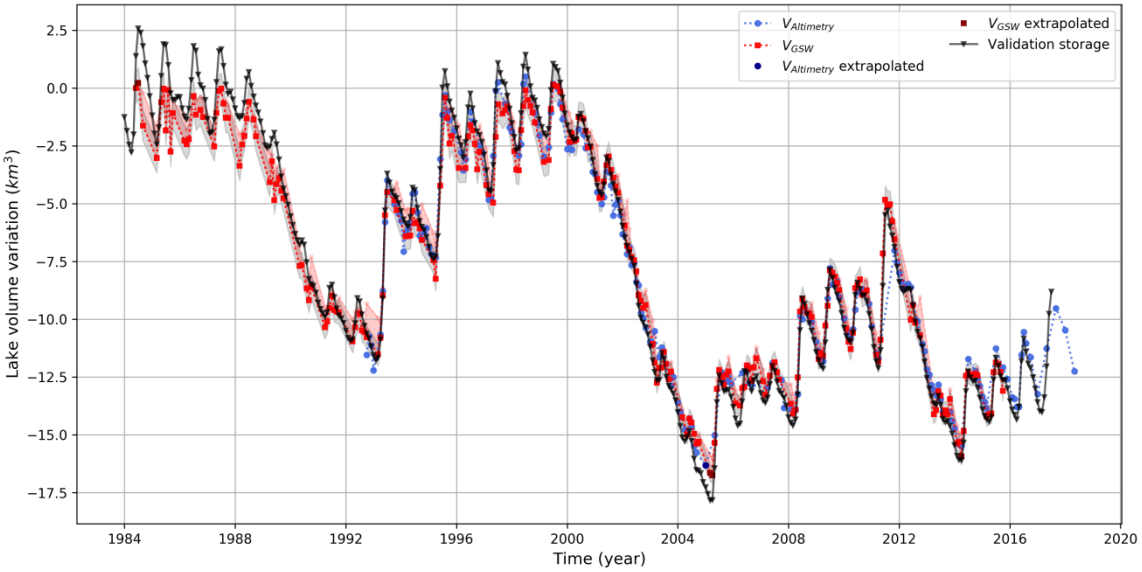

Fig. 4. Validation time series plotted with estimated reservoir volumes for Lake Powell. The black triangle line represents the validation storage as measured using the full lake bathymetry.

Response to RC2 by Anonymous Referee #2

After reviewing the paper of lake volume analysis using satellite altimetry, it is found the topic is good and is of great practical interest, because the determination the relationship between volume and water level is very important for reservoir operation and for rational water allocation. The methods employed in the study are also good compared with the traditional methods by surveying. It will become popular for the estimation of lake volume in the remote region, such as mountain rgion. Therefore, it is recommended to publish in the journal.

Thank you for your interest in our paper and positive comments.

Response to RC3 by Renata Romanowicz

Thank you for your time and interesting comments about our paper.

It is an interesting paper that promotes the use of remote sensing data. It is also well written and well organised. The authors claim that their study can be useful in the assessment of changes in water availability due to climate change. However, I cannot see how the latter can be achieved based on the material presented. The authors are asked to expand on that thought. In addition, I am not sure how this publication might contribute to the enhancement of knowledge on the physical processes involved. In other words, a link is missing between the paper's main contribution – a new lake and reservoir volume dataset - and the possible applications.

This paper's main aim is to develop an automatic methodology to calculate volume variations with remote sensing, that improves on current monitoring techniques. However, we realized that a more detailed and explicit explanation on the possible applications of the dataset will indeed improve the paper.

Proposed correction: **Therefore, we added a much more detailed explanation of the possible applications that will replace the former 'explanation' on line 5-10, page 17**:

'The lake and reservoir volume dataset developed here will help to better understand the behaviour and operations of lakes and reservoirs. As the number of reservoirs is still increasing because of growing energy demands, it is crucial to include their effects in (continental and global scale) hydrological models. Zajac et al. (2017) found that the exclusion of lakes and reservoirs often leads to inaccurate downstream discharge estimates. Furthermore, lake or reservoir storage change combined with modelled or observed inflow allows for a better estimation of the outflow (e.g. Muala et al., 2014). These outflow estimates can be used to calibrate hydrological models or estimate hydropower production in areas where in situ observations are lacking. However, due to a lack of storage observations and their availability – often because of commercial reasons -, the parametrization and the representation of lakes and reservoirs in many hydrological models – if at all present - is still highly simplified. Our global lake and reservoir volume dataset over 32 years will be very beneficial to calibrate and validate their parameterisation to mimic their operational behaviour. This will improve our current understanding of lakes and reservoirs, improve their simulations and consequently the simulations in the rest of the river basin. In addition, a better understanding of reservoirs will also likely improve water and energy production projections of these reservoirs under climate change, or under different management scenarios (e.g. changing downstream water requirements, flow legislation, changing inflow due to other activities upstream). Moreover, the area time series developed in this study can be included in models to improve on (often fixed) current area estimates and can furthermore improve estimates of open water evaporation.'

The authors mention that some lakes showed poor regression between h and A, with one of the reasons being lake size. What are the limits of detection of h(A) relationship from the satellite data (what is the minimum lake area detectable)?

One of the reasons for poor regressions between h and A is indeed lake size. However, as also explained in AC1 and in the discussion section, many other factors induce uncertainty in the regression (e.g. topography around the lakes, lake shape, position of the altimeter track, wave height, ice coverage, time difference between level and area observation, amount of no data in the GSW dataset). Therefore, we did not found a clear relationship between lake size and the R^2 of the regression. A hard limit on the minimum lake size for which the regressions are accurate is hard to give, as it thus depends on many other factors. However, we observed two lakes with an area < 10 km^2 (Barragem do Caia and Encoro de Salas) that still showed accurate regressions. For these lakes the surrounding conditions were ideal and above mentioned uncertainties had a limited influence.

Proposed correction: **We will add the following sentences in line 18, page 17**:
'However, many other factors than the size of the water body determine the accuracy of the measurement; also surrounding topography, surface waves, winter ice coverage, the shape of the water body and the position of the altimeter track determine the measurement error. This could explain why no clear relationship between lake size and regression accuracy (R^2) was observed. Although most lakes with an area < 10 km^2 showed poor regression results, some of these small lakes still returned an accurate regression (e.g. Barragem do Caia and Encoro de Salas). '

From the satellite altimetry data description we learn that the accuracy of water level time series varies with the lake size, from 4-5 cm for large lakes up to over a meter (several decimetres) for small lakes and rivers. Can this variable error variance be included in the calculation of volume variations?

The satellite altimetry data description indeed states that the accuracy for large lakes can potentially be higher than for small lakes. However, as described above and in comment 2 of AC1, the accuracy depends on many other factors. Therefore, we cannot find a relationship between lake size and altimeter accuracy that is clear enough to include the altimetry error in the volume variation estimation.

A global lake and reservoir volume analysis using a surface water dataset and satellite altimetry

Tim Busker[1,2], Ad de Roo[1], Emiliano Gelati[1], Christian Schwatke[3], Marko Adamovic[1], Berny Bisselink[1], Jean-Francois Pekel[1], Andrew Cottam[1]

[1] European Commission Joint Research Centre, Ispra (VA), I – 21027, Italy
[2] Department of Physical Geography, Utrecht University, Utrecht, 3584 CS, the Netherlands
[3] Deutsches Geodätisches Forschungsinstitut der Technischen Universität München (DGFI-TUM), Munich, 80333, Germany

Correspondence to: Tim Busker (tbusker@live.nl) or Ad de Roo (Ad.DE-ROO@ec.europa.eu)

Abstract. Lakes and reservoirs are crucial elements of the hydrological and biochemical cycle and are a valuable resource for hydropower, domestic and industrial water use and irrigation. Although their monitoring is crucial in times of increased pressure on water resources by both climate change and human interventions, publically available datasets of lakes and reservoir levels and volumes are scarce. Within this study, a time series of variation in lake and reservoir volume between 1984 and 2015 were analysed for 1375 lakes over all continents by combining the JRC Global Surface Water (GSW) dataset and the satellite altimetry database DAHITI. The GSW dataset is a highly accurate surface water dataset at 30 m resolution compromising the whole L1T Landsat 5, 7 and 8 archive, which allowed for detailed lake area calculations globally over a very long time period using Google Earth Engine. Therefore, the estimates in water volume fluctuations using the GSW dataset are expected to improve compared to current techniques as they are not constrained by complex and computationally intensive classification procedures. Lake areas and water levels were combined in a regression to derive the hypsometry relationship (dh/dA) for all lakes. Nearly all lakes showed a linear regression, and 42 % of the lakes showed a strong linear relationship with an $R^2 > 0.8$, and an average R^2 of 0.91 and a standard deviation of 0.05. For these lakes and for lakes with a nearly constant lake area (coefficient of variation < 0.008), volume variations were calculated. Lakes with a poor linear relationship were not considered. Reasons for low R^2 values were found to be (1) a nearly constant lake area, (2) winter ice coverage, (3) small lake sizes and (34) a predominance of no data within the GSW dataset for those lakes. Lake volume estimates were validated for 18 lakes in the U.S., Spain, Australia and Africa using in situ volume time series, and gave an excellent Pearson correlation coefficient of on average 0.97 with a standard deviation of 0.041, and a normalized RMSE of 7.42 %. These results show a high potential for measuring lake volume dynamics using a pre-classified GSW dataset, which easily allows the method to be scaled up to an extensive global volumetric dataset. This dataset will not only provide a historical lake and reservoir volume variation record, but will also help to improve our understanding of the behaviour of lakes and reservoirs and their representation in validate (large scale) hydrological models., to improve regional and global flood and drought forecasting systems and to update hydropower estimations.

1 Introduction

Reservoirs and lakes cover a small part of the Earth's land surface (~3.7%, Verpoorter et al, 2014), but are crucial elements in the hydrological and biochemical water cycles. Reservoirs have been constructed at a rapid pace between the 1950s and 1980s, and the construction of new reservoirs will continue over the coming century (Chao et al., 2008; Duan and Bastiaanssen, 2013). Reservoirs therefore have an increasing impact on river discharges, as they are able to alter the hydrograph by storing, retaining and releasing water. They are a valuable resource for hydropower, domestic and industrial water use, wetlands and are the primary water resource for nearly half of the irrigation-based agricultural sector by supplying approximately 460 km^3 of water per year (Biemans et al., 2011; Hanasaki et al., 2006). Moreover, they play a crucial role in biogeochemical activity by emitting vast amounts of CO_2, triggered by CO_2 saturation in lakes and wetlands worldwide (Balmer and Downing, 2011; Cole et al., 2007; Frey and Smith, 2005; Richey et al., 2002).

The amount of water in a reservoir results from the balance of inflow - i.e. direct precipitation, inflowing river discharge, discharge from riparian communities and industries, and subsurface inflow - and outflow - i.e. direct evaporation, withdrawals, reservoir outflow and groundwater percolation - (Duan and Bastiaanssen, 2013). A long-term imbalance can result in considerable reductions in water storage, as frequently observed around the globe in for example Lake Mead, Lake Powell, Lake Poopo and the Aral Sea (Barnett and Pierce, 2008; Micklin, 2016). Reduced water availability in the reservoirs may then result in reductions in hydropower energy production and/or irrigation water availability and lead to economic and societal damage. Many studies have already pointed out that population and economic growth, together with climate change and increasing energy and food requirements will put increasing pressure on water resources (Haddeland et al., 2014; Liu, 2016). A proper understanding of the historical dynamics of reservoirs as a source of water for irrigation, drinking water and energy production, as well as a buffer for flood protection is essential to also improve the quality of future projections on global water resources.

While for individual river basin studies information on reservoirs may be available, especially for larger scale water resource studies at national, continental and global scale, almost no historical records on reservoirs are readily available to run, calibrate and validate hydrological models (Hanasaki et al., 2006). Moreover, in situ lake level and volume measurements are sparse – especially in developing countries – and have even decreased around the globe during last years (Duan and Bastiaanssen, 2013). Even if water levels or volumes are monitored, the information is rarely freely available due to strategic political, commercial or national legislation reasons. Therefore, only a few comprehensive global lake and reservoir data sets exist (e.g. Downing et al., 2006; Lehner and Döll, 2004; Meybeck, 1995; Verpoorter et al., 2014) and if they provide a water storage estimation, these estimates are not dynamic or do not provide data over a longer time series. Therefore, remotely sensed data may be a valuable alternative to monitor water volumes in lakes and reservoirs over the last few decades.

Monitoring lakes and reservoirs using remote sensing has gained much attention over the last few years (e.g. Avisse et al., 2017; Crétaux et al., 2016; Duan and Bastiaanssen, 2013; Frappart et al., 2006b; Gao et al., 2012; Smith and Pavelsky,

2009). Most of these publications focussed on volume variations by combining altimetry water level with lake area from a multispectral sensor. Landsat or MODIS imagery is commonly used to estimate water surface areas, by classifying the satellite images capturing the water body. The classification procedure is demanding and computationally intensive if large areas or many images are classified, and misclassifications may occur because of the diversity of spectral signatures emitted by water surfaces. Therefore, calculating lake areas is often a constraining factor in lake volume calculations. They are predominantly used for the lake hypsometry relationship (dh/dA), but they normally don't provide any temporal details and therefore cannot be used to calculate volume variations on their own (e.g. Duan and Bastiaanssen, 2013; Ran and Lu, 2012; Zhang et al., 2006). Where lakes areas have been calculated to any great extent, this has only been done for a couple of lakes or at a lower resolution (e.g. Smith and Pavelsky, 2009; Tong et al., 2016). Thus, measuring lake volume variations from space is commonly a trade-off between the number of lakes analysed, the resolution of the lake area calculation and the number of historical lake areas that can be calculated. In this study however, by using the pre-processed recently available Joint Research Centre (JRC) Global Surface Water (GSW) dataset with a high temporal and spatial resolution and extensive validation, this trade-off is no longer an issue. Here we perform volume variation estimations globally with a 30 m resolution from 1984 onwards, using all Landsat images available after the launch of Landsat 5. Thereby this study aims to improve on current monitoring techniques and to develop an automatic methodology that is relatively easy to implement at a large scale.

The paper is organized as follows. Section 2 presents the data used in this research, providing a description of the DAHITI altimetry database and an overview of the GSW dataset. Section 3 contains a description of the methods applied, while Sect. 4 gives a description of the results. Section 5 presents a discussion, and finally the conclusions and recommendations are presented in Sect. 6.

2. Data

2.1 Satellite altimetry

Satellite altimetry was initially designed for observing the ocean`s surface. But for more than 10 years now, satellite altimetry has proven to be a suitable tool for measuring water heights of lakes and rivers. Numerous studies have already shown the potential of estimating water level time series over inland waters using different altimeter missions such as Topex/Poseidon (Birkett, 1995), Envisat (Frappart et al., 2006a), Saral (Schwatke et al., 2015b), Cryosat-2 (Villadsen et al., 2015) or ICESat (Zhang et al., 2011). Water levels from satellite altimetry have also been used for hydrological applications such as the estimation of river discharge (Kouraev et al., 2004; Tourian et al., 2017; Zakharova et al., 2006) and lake volumes (Duan and Bastiaanssen, 2013; Tong et al., 2016; Zhou et al., 2016).

Satellite altimetry has the potential to provide reliable water level time series of globally distributed inland water bodies over the last 20 years. ~~However, satellite altimetry is measured only along mission dependent ground tracks. Therefore, larger lakes and reservoirs have a higher probability to be crossed by a satellite track than smaller ones.~~ Topex/Poseidon and Jason-1/-2/-3 have an identical orbit configuration with a 9.9156 days repeat cycle and a track separation of about 300 km at

the Equator. ERS-1/-2, Envisat and SARAL flew on an orbit with a 35 days repeat cycle and a track separation of about 80 km at the Equator. The combination of different altimeter missions is essential to increase the temporal resolution, spatial resolution and length of the water level time series. In order to combine altimeter data from different missions, a mission-dependent range bias resulting from a multi-mission crossover analysis has to be taken into account to achieve long homogenous water level time series (Bosch et al., 2014).

The estimation of water level time series for small lakes, reservoirs or rivers is very challenging. Due to coarse mission-dependent ground tracks with a cross-track spacing of a few hundred kilometres, larger lakes and reservoirs have a much higher probability to be crossed by a satellite track than smaller ones. Moreover, small water bodies tend to have a relatively big altimeter footprint compared to their size, which will affect the resulting shape of the returning waveform. The diameter of the footprint is mainly influenced by the water roughness (i.e. surface waves) and surrounding topography. In reality, the diameter of the footprint can therefore vary between 2 km over the ocean and up to 16 km for small lakes with considerable surrounding terrain topography (Fu and Cazenave, 2001). These land influences and surface waves within the altimeter footprint can affect the altimeter waveforms and require an additional retracking to achieve more accurate ranges. In order to achieve accurate results for small water bodies, the conditions have to be ideal, meaning a low surrounding topography, low surface waves and perpendicular crossings of the altimeter track and water bodies shore. In these ideal cases, satellite altimetry has the capability to observe rivers with a width of about 100-200 m or lakes with a diameter of a few hundred meters. The off-nadir effect is another problem which can occur when investigating smaller water bodies. In general, satellite altimetry measures in the nadir direction, but if the investigated water body is not located in the center of the footprint, then the radar pulses are not reflected in the nadir direction which leads to longer corrupted ranges that must be taken into account (Boergens et al., 2016).

~~The estimation of water level time series for small lakes, reservoirs or rivers is very challenging for satellite altimetry because of the footprint size. In the best case, satellite altimetry has the capability to observe rivers with a width of about 100-200 m or lakes with a diameter of a few hundred meters. Over inland waters, the diameter of the footprint varies between 2 km over the ocean and up to 16 km over land (Fu and Cazenave, 2001). Land influences within the altimeter footprint can affect the altimeter waveforms and require an additional retracking to achieve more accurate ranges. The off-nadir effect is another problem which can occur when investigating smaller water bodies. In general, satellite altimetry is measured in the nadir direction, but if the investigated water body is not located in the center of the footprint, then the radar pulses are not reflected in the nadir direction which leads to longer corrupted ranges that must be taken into account (Boergens et al., 2016).~~

In this paper we use water level time series from the „Database for Hydrological Time Series over Inland Waters“ (DAHITI) as input data for the volume estimation. DAHITI is an altimetry database launched in 2013 by the „Deutsches Geodätisches Forschungsinstitut der Technischen Universität München“ (DGFI-TUM). The data is accessible through a user-friendly web service (http://dahiti.dgfi.tum.de/en/) and is currently providing water levels for more than 780 lakes, reservoirs, rivers and wetlands. The processing strategy of DAHITI is based on a Kalman filtering approach and an extended

outlier detection (Schwatke et al., 2015a) which combines different altimeter missions such as Topex/POSEIDON, Jason-1, 2 and 3, GFO, Envisat, ERS-1 and 2, Cryosat-2, and SARAL/AltiKa. DAHITI uses only high-frequency altimeter data. Depending on the measurement frequency of the altimeter, heights are measured every ~620m (10Hz), ~374m (20Hz), ~294m (18Hz) or ~173m (40Hz) along the altimeter track. To achieve more accurate ranges over inland waters, the Improved Threshold Retracker (Hwang et al., 2006) is used for the reanalysis of the altimeter measurements. The DAHITI approach provides all water level time series error information based on formal errors of the Kalman filtering.

The quality of the water level time series from satellite altimetry in DAHITI has been validated with in-situ data and varies depending on the extent of the inland water body and length of the crossing altimeter track. For large lakes with ocean-like conditions (such as the Great Lakes), ~~an RMS of about 4-5 cm can be achieved. For smaller lakes and rivers an RMS of several decimeters can be achieved.~~ accurate measurements can potentially be achieved with a root-mean-square error (RMSE) as low as 4-5 cm, while for smaller lakes and rivers the RMSE could increase towards several decimeters (Schwatke et al., 2015a). However, no clear relationship was observed between lake size and altimetry accuracy, as the quality of water level time series is not only dependent on the target size, but also on many other factors (e.g. surrounding topography, surface waves, winter ice coverage, the position of altimeter track crossings).

2.2 The JRC Global Surface Water (GSW) dataset

The JRC Global Surface Water (GSW) dataset (Pekel et al., 2016) maps the temporal and spatial dynamics of global surface water over a 32-year period (from 16 March 1984 to 10 October 2015) at 30 m resolution. This dataset was produced by analysing the whole L1T Landsat 5, 7 and 8 archive. At the time of the study, it represented 3066080 images (1823 terabytes of data) and covered 99.95% of the landmass. The analysis was performed thanks to a dedicated expert system classifier. The inference engine of the classifier is a procedural sequential decision tree, which used both the multispectral and multitemporal attributes of the Landsat archive as well as ancillary data layers. It assigned –in a consistent way in both space and time- each pixel to one of three target classes, either water, land or non-valid observations (snow, ice, cloud or sensor-related issues). Classification performance, measured using over 40000 reference points revealed the high accuracy of the classifier; less than 1 % of false water detections, and less than 5 % of omission (Pekel et al., 2016). Thanks to its technical characteristics, the GSW dataset constitutes a very valuable long-term surface water record.

The stack of classified images constitutes the long-term water history documenting the “when and where” of the water presence. This information is recorded in the monthly water history dataset – a set of 380 global scale maps documenting the water presence for each month of the 32-year archive. This monthly information constitutes the most comprehensive and detailed data set of the GSW. Eight additional information layers, documenting different facets of the surface water dynamics are also available within the GSW dataset: (1) water occurrence, (2) occurrence change intensity, (3) seasonality, (4) recurrence, (5) transitions, (6) maximum water extent, (7) monthly recurrence and (8) yearly history. In the framework of this study, the monthly water history and maximum water extent (MWE~~mwe~~)- a map documenting places where water has been detected at least once over the 32 years- were used.

The GSW dataset was completely developed using Google Earth Engine and all of the layers are available through the Earth Engine catalog (Gorelick et al., 2017). Moreover, Earth Engine is used in this research to calculate the monthly lake area time series. Earth Engine is a cloud-based global scale platform optimized for parallel geospatial analyses and data management in earth sciences, using Google's computational power (Gorelick et al., 2017). Earth Engine allowed the analysis of lakes at global scale in high detail, while maintaining a high resolution of 30 m.

3 Methodology

3.1 Calculating monthly lake areas

Monthly time series of lake areas have been calculated for 137~~5~~ lakes over all continents (Figure 1). These contained nearly all lakes available in the DAHITI altimetry database at the time of processing. No additional criteria were set for this study, as the GSW dataset covers all lakes globally. For 380 months over the period 1984-2015 lake areas were calculated using a dedicated Google Earth Engine script. For each lake, a Region of Interest (ROI) was set by a manually drawn polygon that was approximately equal to the ~~mwe~~ MWE of the lake (Figure 2). For every month, lake areas were calculated directly from the GSW monthly history dataset, by counting the number of water pixels inside the polygon and multiplying this by the pixel area. To improve the accuracy of the area calculations, the amount of non-valid observations (no data pixels) within the ~~mwe~~MWE, compared to all ~~mwe~~ MWE pixels within the ROI, has been expressed as the no data fraction. This no data fraction has been used to filter accurate and less accurate area observations in the regression analysis and volume calculations (see Sect. 3.2). The white striping observed for Lake Mead in Figure 2 is an example of no data that is caused by Landsat sensor issues. Moreover, the coefficient of variation (CV) has been calculated from the area observations to express lake area variation normalized by mean lake size.

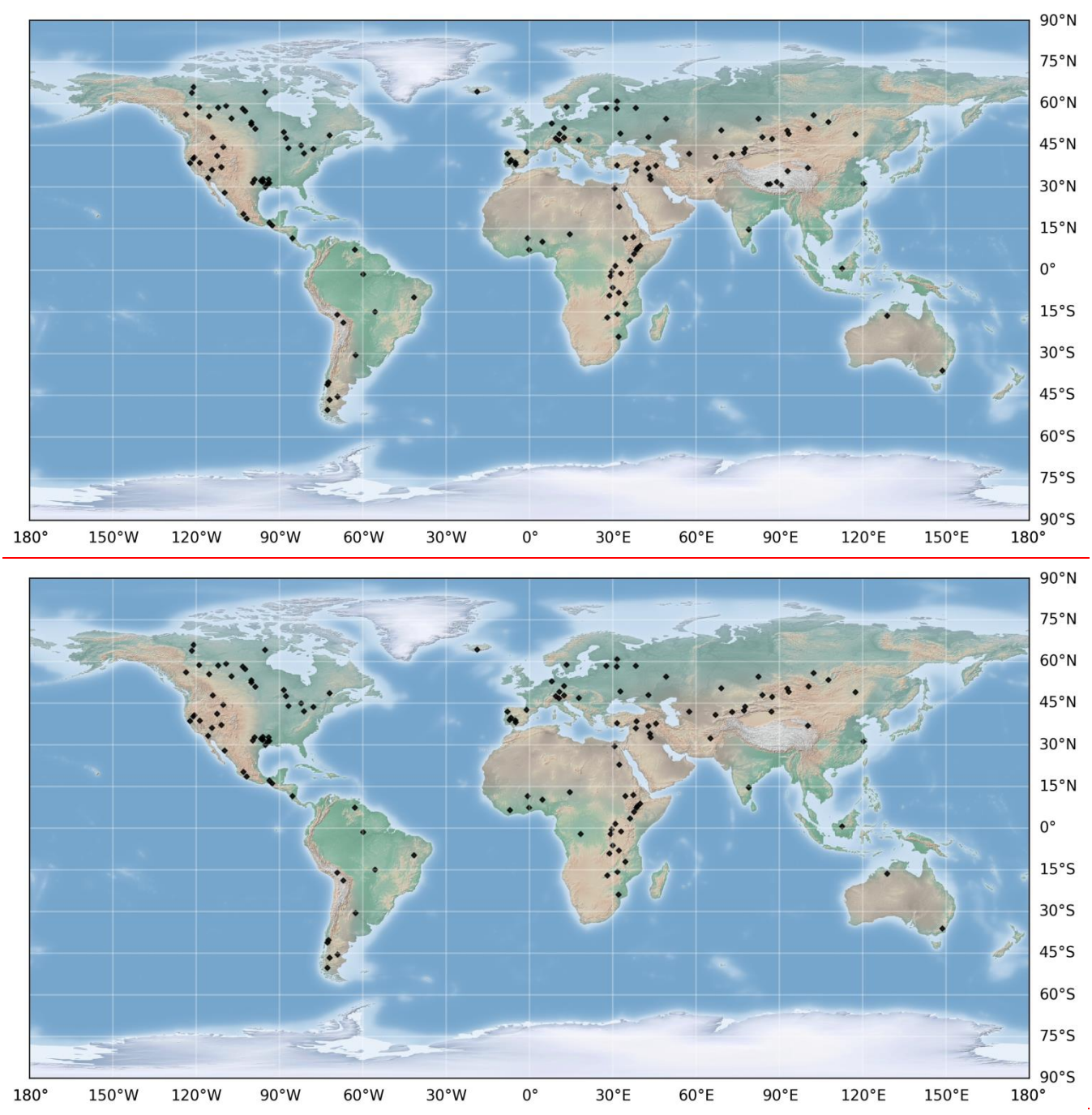

Figure 1 Geographical distribution of the analysed lakes.

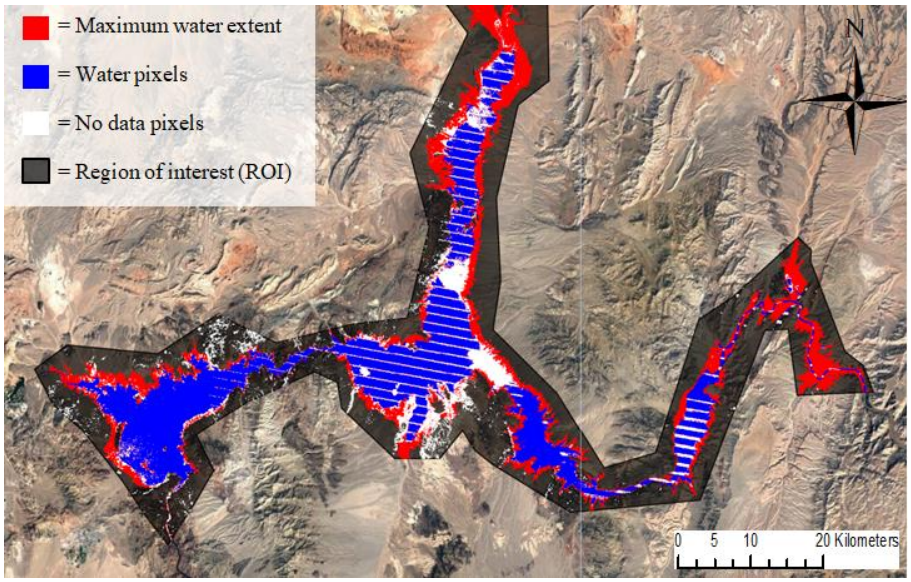

Figure 2 An example of the area input data for Lake Mead (U.S.) for February 2015, where the maximum water extent is marked as red, water as blue and no data as white pixels.

3.2 Calculating lake volumes variations

The volume of a lake or reservoir is a function of the water area (A) and level (h), derived from the hypsometry relationship (dh/dA). Monthly lake areas were only used in the regression if the no data percentage was below 1 %, because only accurate areas were desired to construct the regression line. As exact dates are not provided by the GSW dataset, the altimetry data has first been averaged per month after which monthly water levels ($h_{\text{Altimetry}}$) were coupled with monthly area values (A_{GSW}). These are illustrated with red dots in Figure 3 for Lake Mead (U.S.). The water level-area pairs were assumed to give linear hypsometric relationships of the water bodies (Figure 3, dashed blue line):

$$h_i = a \cdot A_i + b + \varepsilon_i \quad (1)$$

Where A_i and h_i are the area and water level respectively, a and b are the slope and intercept parameters, and ε_i is the error term or residual for time step i. The parameters a and b have been derived by minimising the residual sum of squares (RSS, i.e. $\sum_i \varepsilon_i^2$), using an Ordinary Least Squares Regression (OLS) technique. Therefore, the resulting residuals have zero mean and they are assumed to have a normal distribution. The hypsometric relations can be integrated to obtain the expected volume ~~estimates~~ of the water body:

$$E[V_i] = \frac{(h_i - b) \cdot A_i}{2} \quad (2)$$

Where A_i is the monthly calculated lake area derived from the GSW dataset, h_i is the water level from altimetry and b is the water level of the theoretical lake bottom from the linear regression at A=0, for time step i. By substituting the regression equation in Eq. (2), the expected value of the water volume can be calculated using h or A only:

$$E[V_i] = \frac{(h_i - b)^2}{2a} = \frac{a \cdot {A_i}^2}{2} \quad (3)$$

Subsequently, a confidence interval (CI) was calculated around the expected value of the volumes calculated with A. The residual term in Eq. (1) was included in the volume calculation (Eq. 3) to estimate the residual uncertainty on the expected volumes calculated with A values. It is assumed that the residuals have a zero-mean Gaussian distribution $\varepsilon \sim N(0, {\sigma_\varepsilon}^2)$, where σ_ε is the standard deviation of ε. To obtain the α- probability CI around the expected volume $E[V_i]$, the residual term is replaced by its $\frac{1-\alpha}{2}$ and $\frac{1+\alpha}{2}$ quantiles:

$$CI_{E[V_i]} = \frac{a \cdot {A_i}^2}{2} \pm \frac{A_i}{2} \cdot \sigma_\varepsilon \cdot \Phi^{-1}\left(\frac{1+\alpha}{2}\right) \quad (4)$$

Where $\Phi^{-1}\left(\frac{1+\alpha}{2}\right)$ is the inverse of the cumulative density function of the standardized Gaussian distribution (mean = 0, standard deviation = 1) at probability level $\left(\frac{1+\alpha}{2}\right)$. In this research, a 95 % CI has been used.

Using these equations, absolute volumes are computed by using only the area or water level estimates, giving two different volumetric time series: V_{GSW} and $V_{\text{altimetry}}$. Rather than a 1 % no data threshold in the regression analysis for lake area estimations, a 5 % no data threshold has been applied to area ~~observations~~ estimations used for the volume calculation. This resulted in the best trade-off between the number of observations from the GSW dataset and the accuracy of the estimates. ~~The no data pixels within the mwe have been used to plot an upper limit for the volume estimates, as they could theoretically be water during that specific month.~~

The extrapolated part of the regression line, and therefore in particular the theoretical lake bottom b, should be considered with caution, as the hypsometry relationship may change outside the observational range. The absolute volumes from Eq. (3) are therefore converted to volume variations from t_0 to t_1 (Figure 3, purple area). Most estimated volume variations were calculated using h or A values inside the observed part of the regression line (i.e. inside the range of observed h-A pairs). However, some volumes were estimated with A or h values that are outside such range. These volume estimates use an extrapolated lake hypsometry which is not observed and therefore more uncertain. These estimates are therefore separately classified in the volumetric plots.

Not all lakes showed considerable area fluctuation, as some lakes and reservoirs are artificially bounded or have very steep banks. The signal-to-noise ratio (SNR) for lakes with a very small CV is likely to be low as errors due to no data,

misclassifications and the lake border discretisation with 30 m pixels will mask the actual area variations. Therefore, the areas of lakes with a very small CV were interpreted to be constant. Lake volumes were still calculated, but only by multiplying the mean area with water level variations as observed by altimetry.

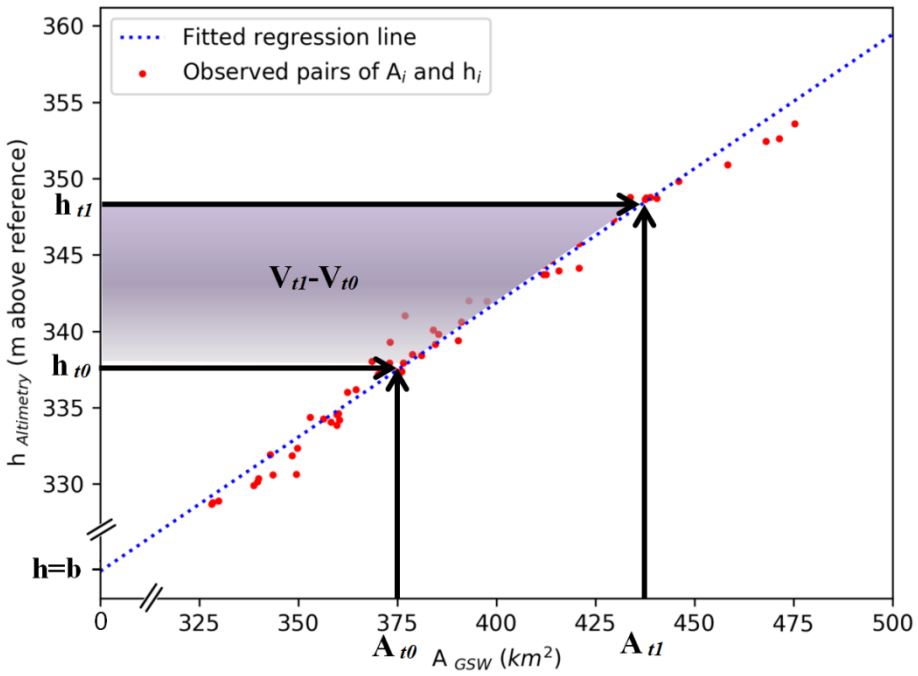

Figure 3 Volume variation calculation for Lake Mead. The observed monthly pairs of *A* and *h* (red dots) are used to estimate a linear regression (blue dashed line) that is used to calculate volumetric changes. The volumetric change from t_0 to t_1 is equal to the purple area and can be visually interpreted as a 2D lake section.

3.3 Validation of the volume estimates

The validation has been carried out using the Pearsons correlation coefficient *r*, the root-mean-square error (RMSE) and the normalized RMSE (NRMSE). The Pearsons correlation coefficient *r* measures the linearity between in situ and estimated volume variations, while the RMSE accounts for the absolute error. The NRMSE has been calculated by normalizing the RMSE with the range of in situ lake volume variations:

$$\mathrm{NRMSE} = \frac{\mathrm{RMSE}}{Obs_{max} - Obs_{min}} \cdot 100\ \% \qquad (45)$$

Where Obs_{max} and Obs_{min} are the maximum and minimum observed in situ volumes since 1984.

4 Results

4.1 Regression analysis

1375 lakes and reservoirs have been analysed over all continents. The linear OLS regression analysis resulted in highly variable R^2 values among the lakes and reservoirs. Low R^2 values were observed to be caused mainly by noise rather than non-linear hypsometry, as only three lakes (Tawakoni, Urmia and Eagle) returned a clear non-linear hypsometry relationship (see discussion). The mean R^2 of all 1375 lakes is only 0.589, but 587 lakes showed an $R^2 > 0.8$ with an average of 0.91. Lake Eucumbene (Australia), Lake Kariba (Zambia), Lake Powell, Lake Mead and Hubbard Creek Reservoir (U.S.) are examples of these lakes, with high R^2 values and low regression residuals. The regression results for Lake Powell, Kariba, Mead and Nasser are showed in Figure 4, with R^2 values of respectively 0.99, 0.96, 0.98 and 0.92.

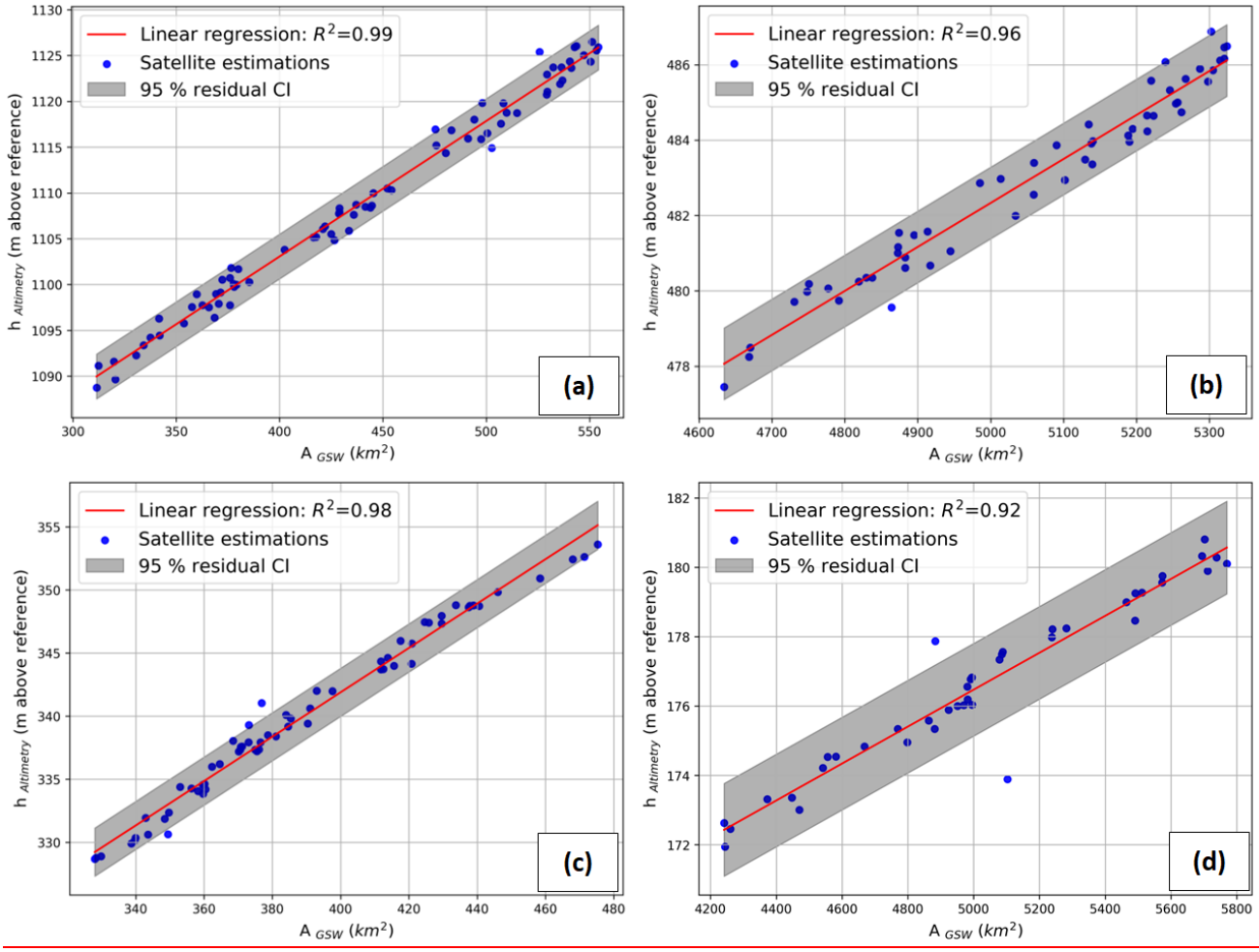
Linear regression: R^2=0.99
Satellite estimations
95 % residual CI
(a)
h Altimetry (m above reference)
A GSW (km^2)
Linear regression: R^2=0.96
Satellite estimations
95 % residual CI
(b)
h Altimetry (m above reference)
A GSW (km^2)
Linear regression: R^2=0.98
Satellite estimations
95 % residual CI
(c)
h Altimetry (m above reference)
A GSW (km^2)
Linear regression: R^2=0.92
Satellite estimations
95 % residual CI
(d)
h Altimetry (m above reference)
A GSW (km^2)

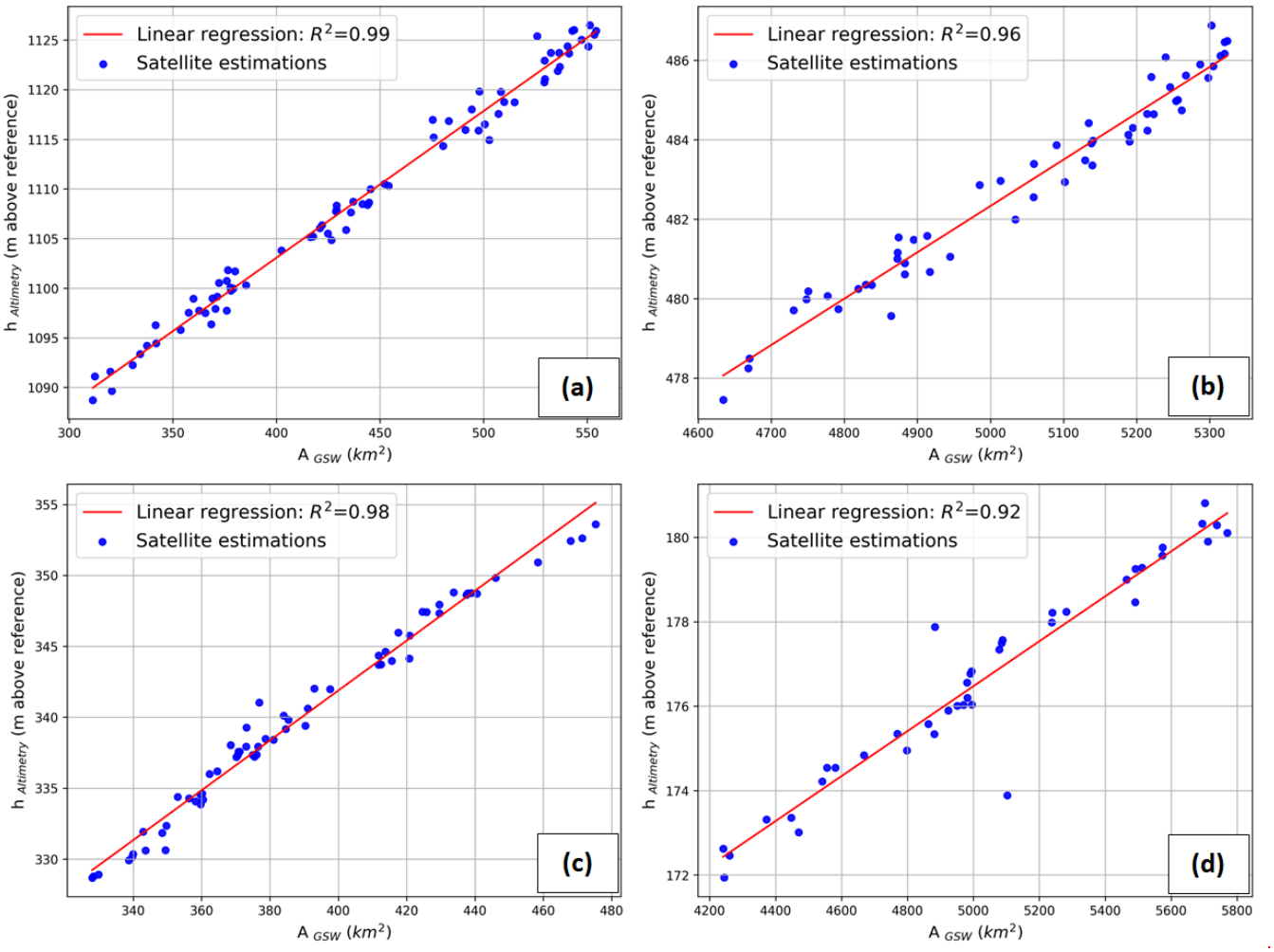

Figure 4 Area-level regressions for Lake Powell (a), Kariba (b), Mead (c) and Nasser (d), with R^2 values of respectively 0.99, 0.96, 0.98 and 0.92.

4.2 Division of the lakes in groups

Based on the R^2 values from the regression and the area CV, the lakes have been subdivided into lakes with a constant area (Lc) and lakes with a variable area (Lv) where the latter (Lv) category has been further subdivided into lakes with a good performance (LvG; $R^2 > 0.8$) and lakes with a poor performance (LvP; $R^2 < 0.8$) (Figure 5). 421 lakes are categorized as Lc as they showed a CV < 0.008 and all these lakes returned a $R^2 < 0.6$ with an average of 0.16 (black circles, Figure 5). These lakes have a very small variation in area, resulting in highly inaccurate regressions due to a low SNR. Therefore, these lakes were assumed to have a constant area and their volume was calculated by multiplying water level observations with the average of the GSW area estimates. For CV > 0.008, lakes showed considerable monthly area variations and mostly acceptable R^2 values with an average of 0.76. 587 lakes where classified as LvG as they showed a $R^2 > 0.8$, with an average

of 0.91 (green triangles, Figure 5). For these lakes, volumes have been calculated using accurate linear regressions. For 375 lakes with a variable area, the regression was less accurate with a $R^2 < 0.8$ and a mean of 0.502 and therefore they are classified as LvP (red triangles, Figure 5). A table for each group, showing the most important lake properties and the R^2 values, is given in appendix 1.

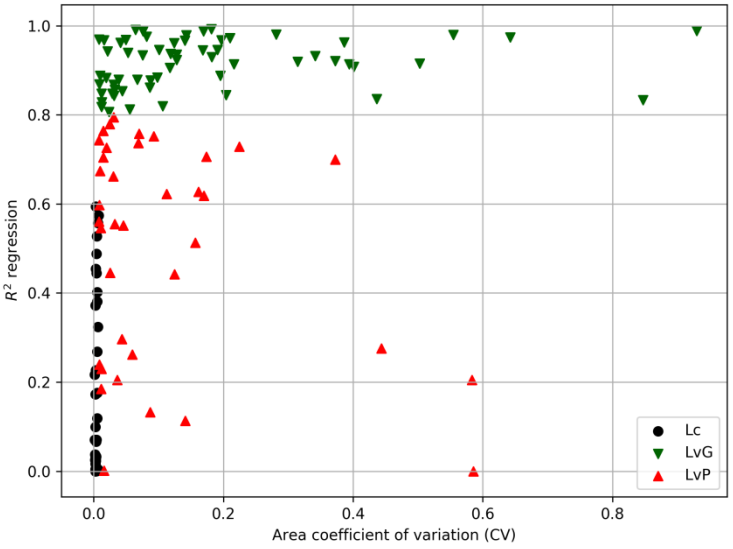

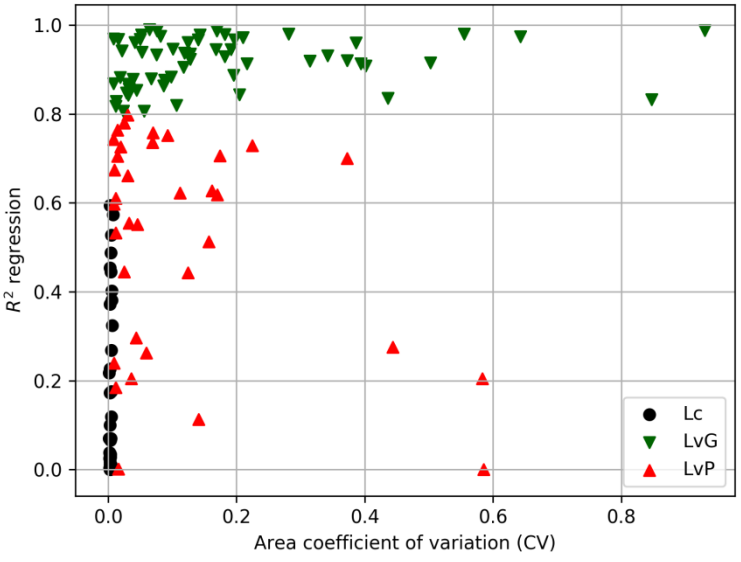

Figure 5 Illustration of the division of the lakes into lakes with a constant area (Lc) and a variable area with a good performance (LvG) and with a poor performance (LvP), based on the R^2 and CV values.

4.3 Volumetric results

For a total of ~~98~~ 100 lakes (5~~8~~7 variable area lakes and 4~~2~~1 constant area lakes), the volume variation time series have been calculated, using both water levels ($V_{Altimetry}$) and water areas (V_{GSW}) as inputs. Volumetric results of the variable area lakes Powell, Kariba, Mead and Nasser are outlined below and are shown in Figure 6. $V_{Altimetry}$ or V_{GSW} estimates inside the observational range of the regression (*h*-*A* pairs) are coloured blue and red. Some volume estimates are derived from observations outside the regression range; these are extrapolated estimates and are displayed with a darker colour tint. The red line displays the best estimate of the volume variation as calculated with observed water classifications in the GSW dataset (i.e. total area of surface water). The red shaded area displays the upper volume boundary on the V_{GSW} estimates, as derived from the GSW dataset pixels classified as no data within the MWE (max 5 %, see section 3.2). These no data pixels could theoretically be covered with water for that month, and this would increase the estimated volume. In this case the volume variation estimate would be somewhere within the red shaded area. The upper limit of the red shaded area would thus be reached if all no data pixels within the MWE contain surface water during that particular month. Another source of uncertainty is the uncertainty induced by the residuals in the regression, which is represented by the grey shaded area. It shows the effect of the 95 % residual-based CI on the volume variation estimates as calculated with Eq. (4). ~~The light red shaded areas display the uncertainty interpolated from the 5 % no data pixels in the area estimate and how this no data propagates to the volume estimate. It represents pixels which theoretically could be water, but that were not observed due to the presence of no data within the mwe.~~

Figure 7 summarizes the volumetric results, by showing lake location, lake type (constant, variable good or variable poor lakes), and the average volumetric change. The volumetric change shows the magnitude of reduction (red circles) or increase (blue circles) of average water storage between the periods 1984-2000 and 2000-2015 for LvG, and from 2000-2008 to 2008-2016 for Lc. Slightly more lakes showed a positive change (60~~59~~) than a negative one (40~~37~~). Considerable reductions of water storage were observed in Western U.S., due to major average volume declines in Lake Mead (10 km^3), Powell (6 km^3) and the Great Salt Lake (16 km^3). Average increases were found for the Great Lakes and most of the analysed lakes in Southeast Africa.

Lake Mead was formed after the construction of the Hoover Dam during the 1930s, in the former steep V-shaped slopes created by the Colorado River. It is located approximately 50 km east of Las Vegas in the Black Canyon, Arizona- Nevada (Figure 7). With a maximum depth of 158 m and a maximum capacity of 33-35 km^3, Lake Mead is the largest reservoir in the U.S. by capacity and the second largest (after Lake Powell) by water area (Barnett and Pierce, 2008; Holdren and Turner, 2010). The lake showed a considerable reduction in water storage between 1984 and 2015 (Figure 6c). Between two periods of maximal reported capacity (1984-1988 and 1998-2000), a small decrease in capacity of around 7 km^3 was observed. From its historical maximum capacity in 2000, the water level dropped 40 m between 2000 and 2010 (Cook et al., 2007; Duan and Bastiaanssen, 2013), mainly because of a combination of water abstractions by around 25 million people and multiple intensive droughts (Holdren and Turner, 2010). This reduction of water storage is also reported by the satellite estimates.

According to our estimates, Lake Mead lost approximately 20 km^3 of water from 2000 to 2015 (Figure 6c, Figure 7). Using the USGS in situ measurement of storage volume of 31 km^3 in 2000, this is an almost 70 % reduction of water storage over the last 15 years.

Lake Nasser is a crucial resource for Egypt's population, functioning as a source for irrigational water and electricity and as an important flood-control mechanism. With an estimated maximum storage capacity of 162 km^3, Nasser is the main freshwater resource for approximately 85 % of the Egyptian population (Gao et al., 2012; Muala et al., 2014). The lake shows a strong annual cycle, with declines in water storage during the first half of the year and increases during the second half of the year (Figure 6d). The annual cycle amplitude varies from around 10 to 20 km^3. Besides this yearly fluctuation, Lake Nasser features an even longer inter-annual variability. From the lowest recorded volume over 1985-1993, water storage increased at least 40 km^3 to record-high estimates in the period 1998-2002. From 2002, the lake shows a decreasing trend towards 2006~~, in which it lost~~, during which time it lost approximately 30 km^3. Two peaks were observed over 2007-2009 and in 2005, when the lake gained 30-35 km^3 of water and subsequently lost the same amount. The lake showed an average volume decrease over the whole observational period of only 1.8 km^3, which is negligible compared to the size of the lake (Figure 7).

Lake Kariba formed after the construction of the Kariba Dam on the Zambezi River on the border of Zimbabwe and Zambia (Berg et al., 1996). It has an average surface area of 5364 km^2 and with an estimated capacity of 185 km^3 it is the largest reservoir in Africa by volume (LakeNet, 2003). The reservoir shows a consistent seasonal variation, with increases of around 10-20 km^3 during the first five months, and decreases over the last seven months of the year (Figure 6b). Moreover, the lake gained at least 45 km^3 of water from 1996 to 1999. From 2000 to 2007, the volume decreased again by approximately 30 km^3. From 2008, the water volume increased to a maximum reported capacity in May 2010. From July 2014, the lake shows a constantly decreasing trend towards the last year of the data (September 2015). Over the whole observational period, the average storage of the lake increased by 15 km^3 (Figure 7).

With an area of 653 km^2, Lake Powell is the largest lake in the U.S. by water surface area (Barnett and Pierce, 2008; Benenati et al., 2000). Its maximum capacity of 33.3 km^3 is slightly less than that of Lake Mead (Benenati et al., 2000; Holdren and Turner, 2010). The lake showed two periods of maximum capacity during 1984-1988 and 1995-2000 (Figure 6a). As observed for Lake Mead, a period of intensive drought in the years after 2000 caused a considerable reduction in volume. Over the period 2000-2004, water storage declined by approximately 16 km^3. According to Cook et al. (~~,~~2007), the volume left was only 38 % of the live capacity. The average volume decreased by 6.3 km^3 from 1984-2000 to 2000-2015 (Figure 7).

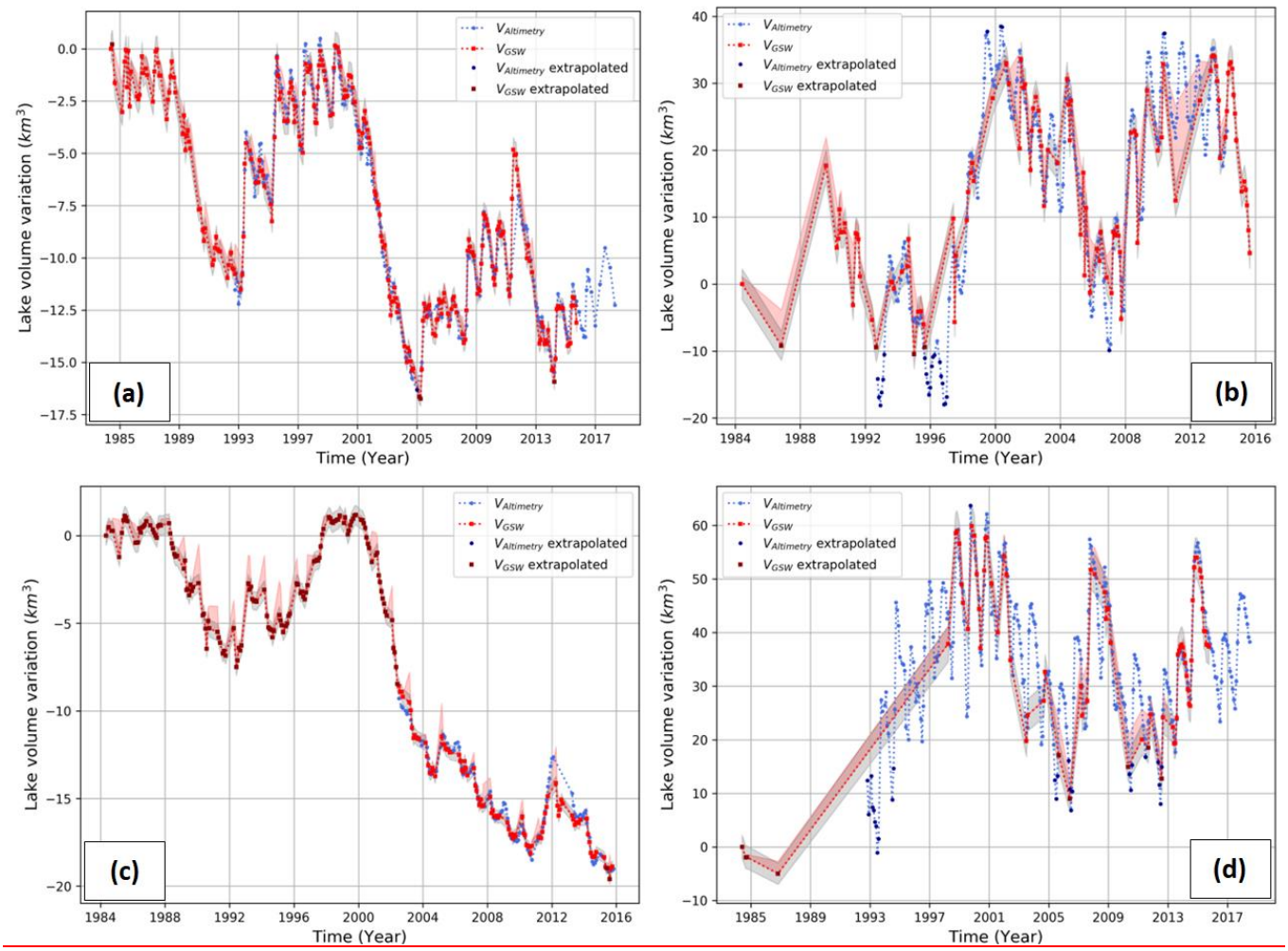
(a)
(b)
(c)
(d)
Lake volume variation (km^3)
Time (Year)
$V_{Altimetry}$
V_{GSW}
$V_{Altimetry}$ extrapolated
V_{GSW} extrapolated

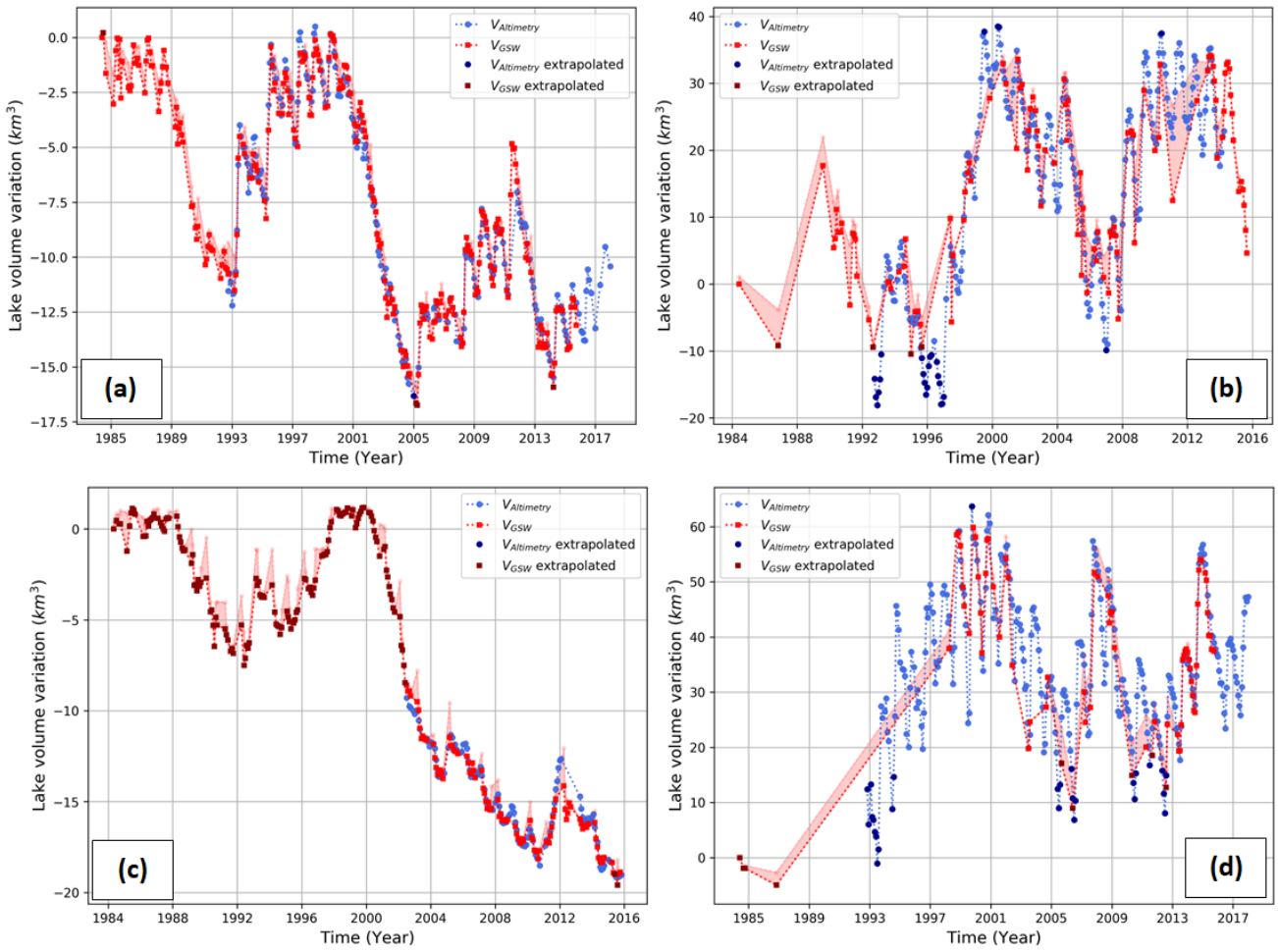

Figure 6 Lake volume variations for Lake Powell (a), Kariba (b), Mead (c) and Nasser (d) using $V_{Altimetry}$ (blue) and V_{GSW} (red). **The grey and red shaded areas represent the 95 % residual-based CI and the uncertainty induced by the no data within MWE, respectively.**

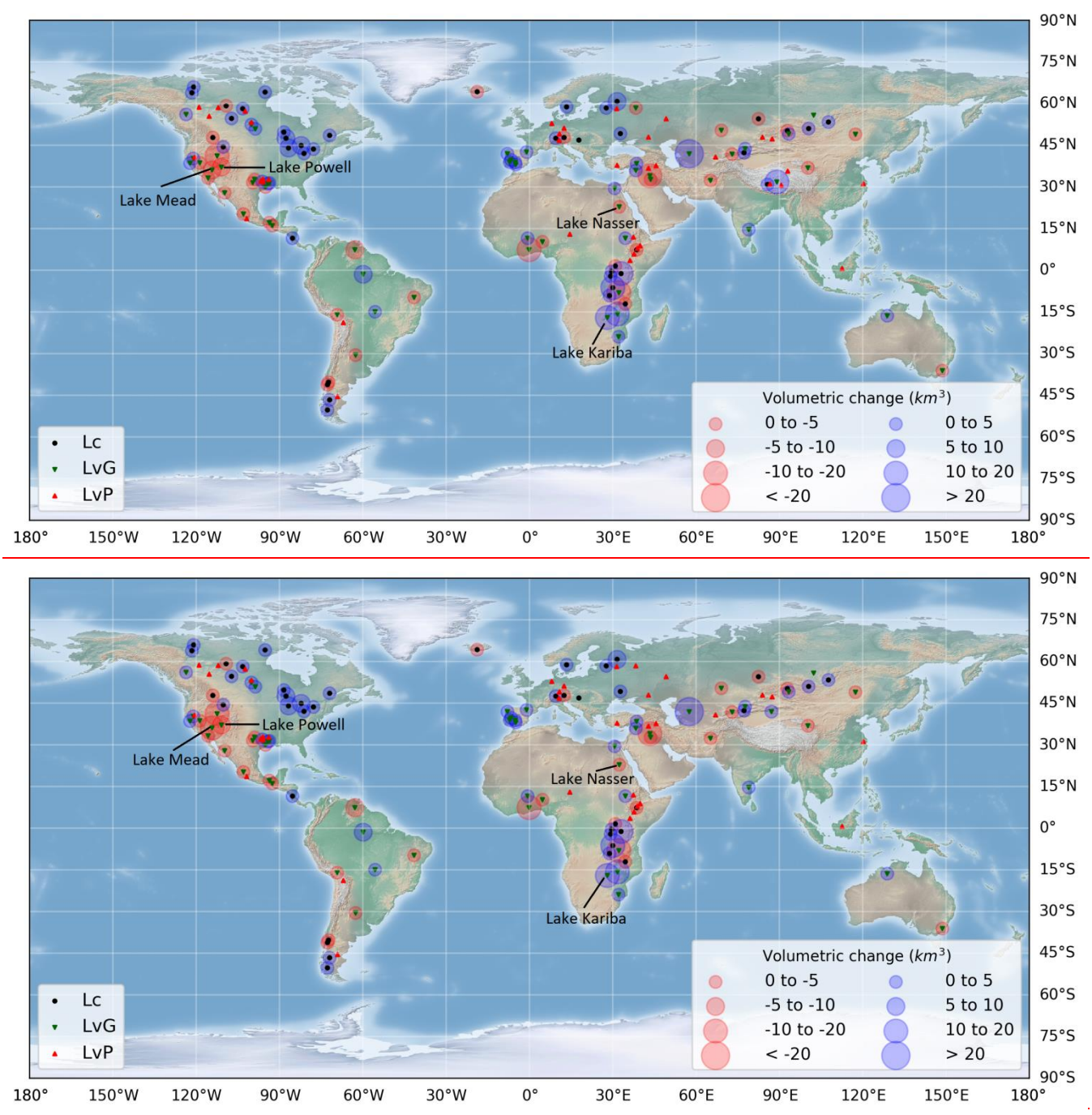

Figure 7 Lake and reservoir types (constant (Lc), good variable (LvG) or poor variable (LvP)) with the average volume change.

4.4 Validation of the volume estimates

Lake volume variations have been validated against in situ data that are based on a full bathymetric survey for 18 lakes. Nine of these lakes are located in the USA (Richland Chambers Reservoir, Hubbard Creek Reservoir, Lake Mead, Lake Houston, Lake Powell, O. H. Ivie Lake, Toledo Bend Reservoir, Lake Walker and Lake Berryessa), 1 in Africa (Roseires Reservoir), 6 in Spain (Serena Reservoir, Puente Nuevo Reservoir, Alcantara Reservoir, Lake Almanor, Yesa Reservoir and Encoro de Salas Reservoir) and 2 in Australia (Lake Argyle and Lake Eucumbene). U.S. lakes have been validated using USGS in situ lake/reservoir volumes obtained from: https://waterdata.usgs.gov/nwis/current. Lake Powell was the only U.S. reservoir whose data were obtained from the United States Bureau of Reclamation (USBR): https://www.usbr.gov/rsvrWater/HistoricalApp.html. Spanish validation data were gathered from the Spanish Ministry of Agriculture, Food and Environment via http://ceh-flumen64.cedex.es. In situ data for Roseires Reservoir were received from the Dams Implementation Unit of Ministry of Water Resources and Electricity, Sudan. Validation data for Lake Argyle and Lake Eucumbene were obtained from WaterNSW in Australia via http://realtimedata.water.nsw.gov.au/water.stm.

The validation analysis has been done for volumes both excluding and including extrapolation. The non-extrapolated volumes showed average Pearsons *r*, RMSE and NRMSE of 0.96, 0.14 km^3 and 7.25 % respectively (Table 1). The high correlation indicates that the validation data showed a very high linearity. ~~The average NRMSE is relatively low taking into account all sources of uncertainty~~. When the extrapolated volumes ~~are~~ were included, the NRMSE ~~is~~ was ~~only~~ slightly higher (7.4 %), but still acceptable for most lakes. However, for *h* or *A* observations that are much smaller or larger than the observed *h*-*A* pairs in the regression, the extrapolation errors can be much higher (e.g. Roseires Reservoir). In general, relatively few V_{GSW} or $V_{Altimetry}$ estimates used this extrapolation.

Figure 8 shows the relationship between satellite and in situ volume variations for Lake Mead and illustrates the accuracy of the methodology. The estimates showed strong linearity with in situ data, as shown by the correlation coefficient of > 0.99 for both V_{GSW} as $V_{Altimetry}$. Both estimates ~~are~~ were very close to the 1:1 line and therefore ~~have~~ had a low NRMSE of 5.43 and 1.87 for V_{GSW} and $V_{Altimetry}$ respectively. The NRMSE of V_{GSW} ~~is~~ was slightly higher, as this includes the extrapolated volume estimations from volume variations of 2 to -8 km^3. These volumes were estimated using area observations outside the range of *h*-*A* pairs used in the regression. It is clear that the hypsometry of the lake does not hold perfectly true for these calculated areas.

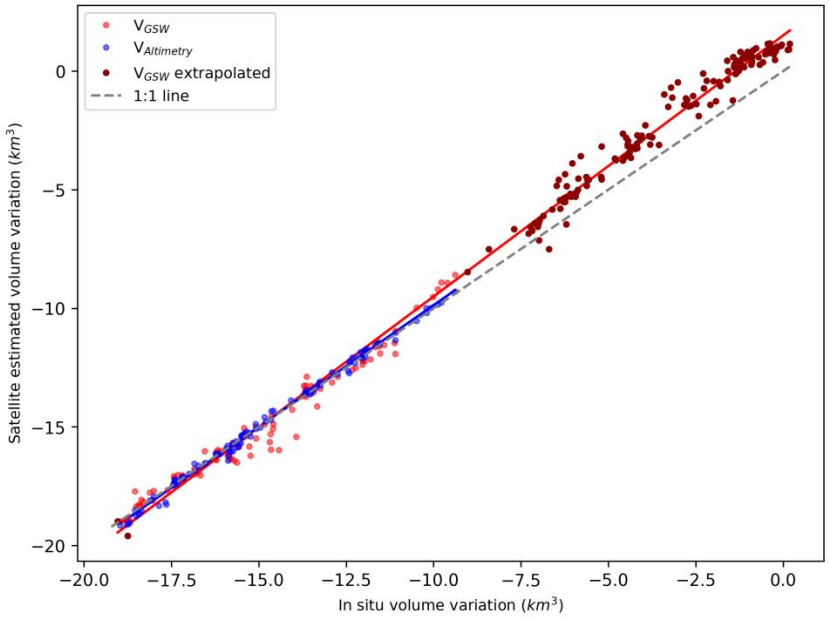

Figure 8 Relationship in volume variation between satellite estimated and in situ observations for Lake Mead, with a Pearsons *r* > 0.99 and a NRMSE of 5.43 % (V_{GSW}) *and* 1.87 % ($V_{Altimetry}$).

Figure 9~~Figure 10~~ and Figure 10 show the validation volume time series against the satellite estimated volumes for Lake Mead and Lake Powell respectively. The time series showed that both the timing and magnitude of the estimated volume fluctuations ~~are~~ were accurate for these lakes. For the non-extrapolated part of Lake Mead (2002-2016), estimated volumes were almost equal to the validation data. The extrapolated part (before 2002) was slightly overestimated. However, the dynamics over this period ~~are~~ were still well captured. Lake Powell also showed accurate results, for both the seasonal and inter-annual fluctuations in water storage. Noteworthy for both lakes is the density of area observations due to a low amount of no data in the GSW dataset. For Lake Powell, the V_{GSW} even correctly captured seasonal fluctuations, which is not always the case (see discussion). The high accuracy ~~is~~ was expressed in a low NRMSE of 4.52 and 2.96 % for V_{GSW} and $V_{Altimetry}$ respectively. Note that almost no extrapolated volume estimates were required for the volume time series of Lake Powell.

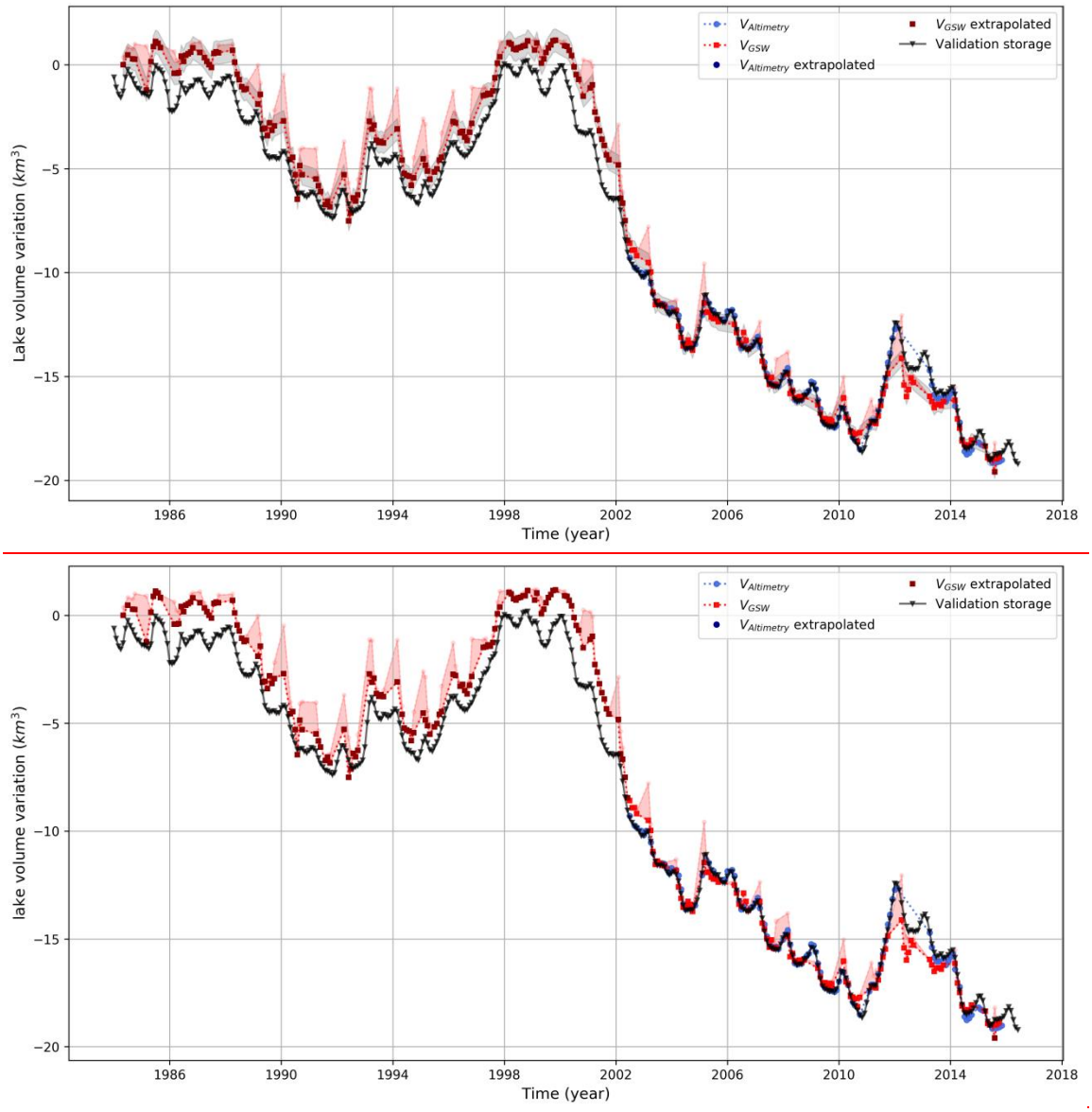

Figure 9 Validation time series plotted with estimated reservoir volumes for Lake Mead. The black triangle line represents the validation storage as measured using the full lake bathymetry. The grey and red shaded areas represent the 95 % residual-based CI and the uncertainty induced by the no data within MWE, respectively.

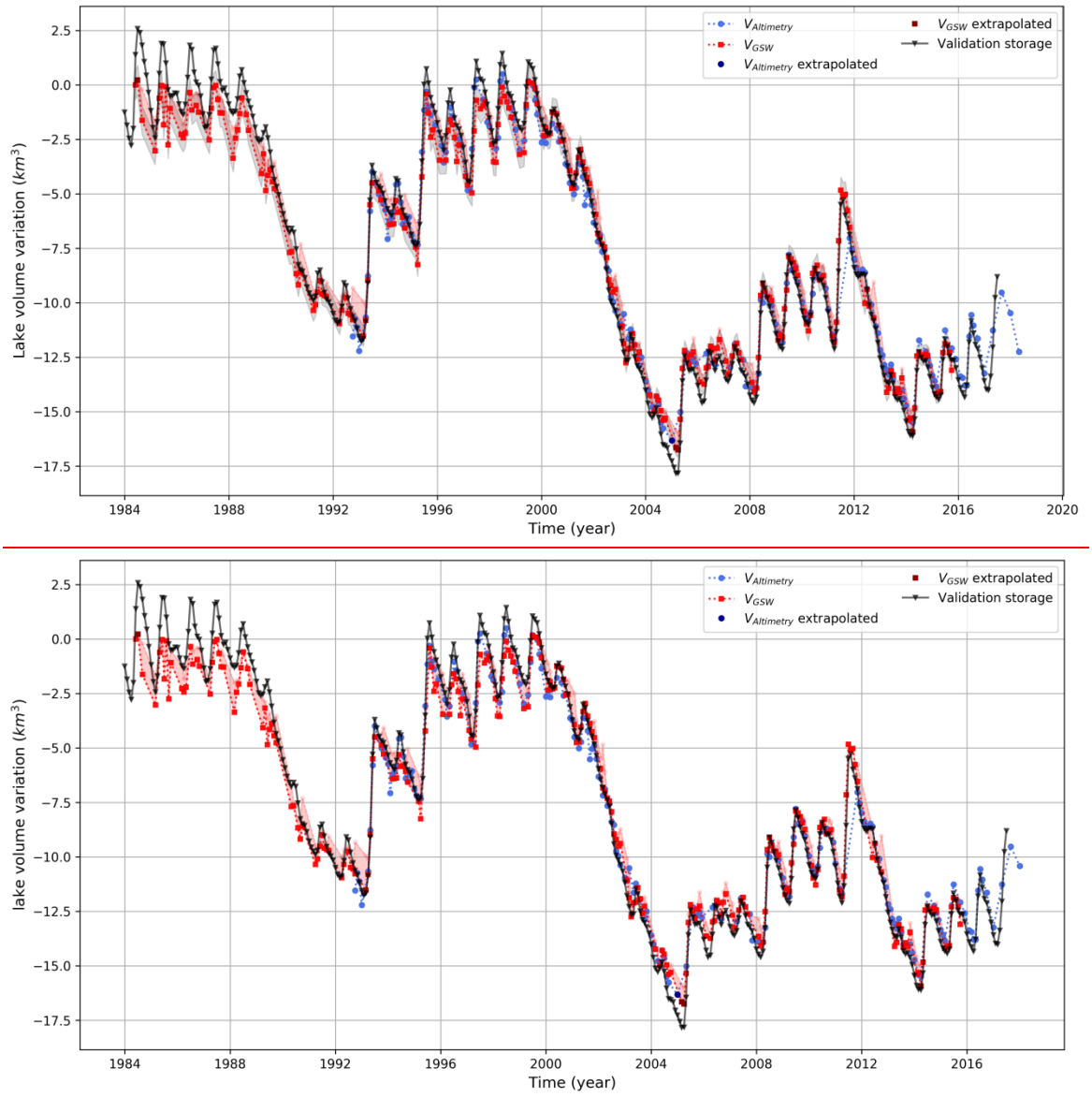

Figure 10 Validation time series plotted with estimated reservoir volumes for Lake Powell. The black triangle line represents the validation storage as measured using the full lake bathymetry. The grey and red shaded areas represent the 95 % residual-based CI and the uncertainty induced by the no data within MWE, respectively.

5. Discussion

This study presented a new methodology to estimate lake and reservoir volumes using remote sensing alone. The validation showed that the method can produce water storage change estimates for many lakes, thus highlighting the

potential of combining satellite altimetry and the GSW dataset to develop a global lake and reservoir volume variation dataset. The GSW dataset global coverage, 30 m resolution, high accuracy and monthly surface water observations over a 32-year period increases the number of analysed lakes and the accuracy, quantity and temporal range of lake area calculations. Therefore, volume variations can now also be calculated using GSW lake areas as input independent from altimetry data, which allows for volume calculations further back in time to 1984. ~~The lake volume variations estimated here are likely to be useful in unravelling the causes of changing water availability due to climate change, extreme climate phenomena such as El Niño and La Niña, human abstractions and reservoir construction and operations. The volume estimations can help to validate large scale hydrological models and thus to improve future projections. Also, understanding volumetric lake and reservoir changes will be beneficial for regional and global flood and drought forecasting systems. Finally, hydropower estimations may also be improved using these data.~~

The lake and reservoir volume dataset developed here will help to better understand the behaviour and operations of lakes and reservoirs. As the number of reservoirs is still increasing because of growing energy demands, it is crucial to include their effects in (continental and global scale) hydrological models. Zajac et al. (2017) found that the exclusion of lakes and reservoirs often leads to inaccurate downstream discharge estimates. Furthermore, lake or reservoir storage change combined with modelled or observed inflow allows for a better estimation of the outflow (e.g. Muala et al., 2014). These outflow estimates can be used to calibrate hydrological models or estimate hydropower production in areas where in situ observations are lacking. However, due to a lack of storage observations and their availability – often because of commercial reasons -, the parametrization and the representation of lakes and reservoirs in many hydrological models – if at all present - is still highly simplified. Our global lake and reservoir volume dataset over 32 years will be very beneficial to calibrate and validate their parameterisation to mimic their operational behaviour. This will improve our current understanding of lakes and reservoirs, improve their simulations and consequently the simulations in the rest of the river basin. In addition, a better understanding of reservoirs will also likely improve water and energy production projections of the influence of these reservoirs under climate change, or under different management scenarios (e.g. changing downstream water requirements, flow legislation, changing inflow due to other activities upstream). Moreover, the area time series developed in this study can be included in models to improve on (often fixed) current area estimates and can furthermore improve estimates of open water evaporation.

The methodology used in this study has a couple of limitations. They arise mainly from limitations in the input data (GSW and DAHITI altimetry dataset) and the volume calculation methodology.

5.1 Satellite altimetry limitations

The altimeter footprint can be up to 16 m over land and land influences inside this footprint can alter the water level accuracy by disturbing the altimeter waveforms (Fu and Cazenave, 2001). Water level estimations of very small lakes or reservoirs can therefore have a RMSE of several decimeters or larger (Schwatke et al., 2015a). We analysed many small

lakes in Europe that did not show accurate regressions when they were relatively small (e.g. Thülsfelder Talsperre, 1.7 km^2, Hainer See, 4 km^2, Lake Resia, 6.6 km^2 and Altmuehl See, 4.5 km^2). However, many other factors than the size of the water body determine the accuracy of the measurement; also surrounding topography, surface waves, winter ice coverage, the shape of the water body and the position of the altimeter track determine the measurement error. This could explain why no clear relationship between lake size and regression accuracy (R^2) was observed. Although most lakes with an area < 10 km^2 showed poor regression results, some of these small lakes still returned an accurate regression (e.g. Barragem do Caia and Encoro de Salas). ~~Moreover, water~~Water level estimations are only possible if the water body is located along mission-dependent ground tracks. Larger lakes and~~or~~ reservoirs were more frequently captured by a combination of satellite tracks and therefore showed more frequent observations than smaller ones. ~~have a higher probability of frequent observations and a higher accuracy than smaller inland water bodies.~~

5.2 The influence of no data in lake area calculations

The classifier of the GSW dataset has been shown to be very accurate, with less than 1 % of false water detections, and less than 5 % omission (Pekel et al., 2016). Therefore, the influence of classification errors in the volume estimations was very limited.

In this methodology, no data classifications in the GSW dataset play a much more important role. These are caused by snow, ice, cloud or sensor-related issues (e.g. white striping in Figure 2) and are likely to give an underestimation of the actual lake area if they are inside the ~~mwe~~MWE. Therefore, their influence has been reduced with strict no data thresholds applied to each monthly calculation. The 1% no data threshold for the regression and 5 % for the volume calculation resulted in the best trade-off between the number of observations from the GSW dataset and the accuracy of the estimates. Higher no data thresholds introduced too much variability in the volume estimates, as (1) regression lines became much noisier and (2) the area of monthly no data exceeded the actual lake area variation. Locations with frequent cloud cover, lake ice coverage or sensor-related image failures will often return no data amounts that exceed the threshold, resulting in a sparse V_{GSW} time series. Although they are sparse, these area volume estimates can still show an acceptable accuracy, as was observed for the Puente Nuevo Reservoir in Spain (Figure 11). For locations in the high or low latitudes, winter months are masked due to low solar zenith angles that cause considerable shadowing. Moreover, a short period of daylight or ice and snow coverage on the water surface can further increase the amount of no data in these regions.

Besides the varying image quality, the whole stack of historical Landsat imagery has an unequal global spatial distribution. The U.S. and Australia are well covered, while other regions, like Africa and Southwestern Europe, have much less Landsat observations (Pekel et al., 2016; Wulder et al., 2016). The volumetric plots of U.S. lakes therefore typically show a highly dense V_{GSW}, while lakes in Africa and other less monitored regions typically have more years of no observations, especially before 2000. This can clearly be observed by comparing Lake Mead and Powell (U.S.) with Lake Nasser and Kariba (Africa) in Figure 6. However, for lakes with sparse V_{GSW} estimates, $V_{Altimetry}$ estimates still provide a valuable volume variation record.

Many layers in the GSW dataset could be used to reduce the amount of no data pixels. This would considerably increase the capabilities of the methodology, especially in the regions mentioned above. No data pixels that are located in the middle of the lake and are surrounded by water pixels (e.g. Figure 2) have a high probability of being water. Furthermore, the large temporal range (1984-2015) of the GSW dataset could be used to further decrease the amount of no data. For example, no data pixels that are classified as water over nearly all the 380 months could be assigned to the water class with high confidence. The GSW seasonality layer could also be used to find permanent water pixels, which can be converted to water if they are not observed during a specific month.

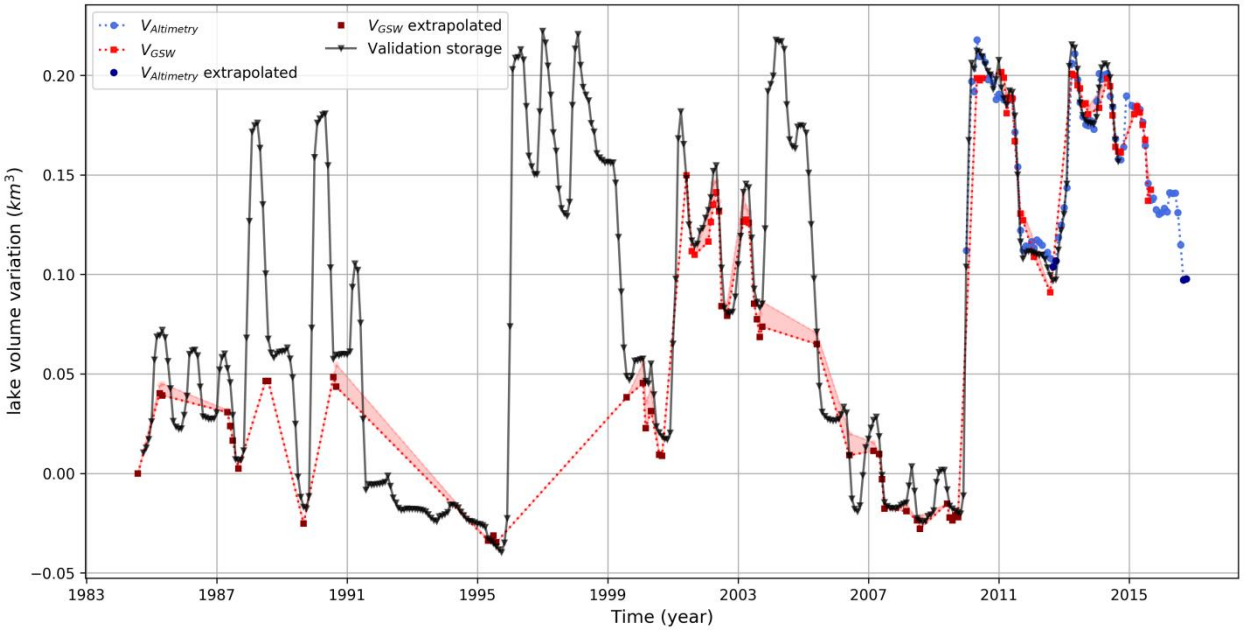

Figure 11 Time series of satellite estimated volume variations compared to validation storages for Puente Nuevo Reservoir.

5.3 Uncertainties and limitations in the volume calculation technique

Only three out of 13~~75~~ lakes (Tawakoni, Urmia and Eagle) ~~gave~~ showed a clear non-linear area-level relation. ~~hypsometry relationship and~~ For these lakes, volume variations were not estimated. ~~for these lakes volumes are assumed to be unreliable~~. Their regressions could be explained by a second- or third-order polynomial, as shown for Lake Urmia in Figure 12. This non-linearity is caused by a considerable change in slope, which will mostly be observed for lakes with extremely low water levels (e.g. Lake Urmia) or during floods.

To reduce data size, the monthly GSW dataset does not include exact dates of the Landsat observations. This causes more uncertainty in the regression, as the level and area observations may refer to different dates (maximum difference of one month) and therefore to slightly different lake conditions. For lakes with a highly variable level within a month, this uncertainty therefore increases. The outliers in the regression of Lake Nasser (Figure 4d) are expected to be largely induced by this uncertainty. For both outliers, the altimeter measurements were taken in the beginning of the month (2th and 6th

day), and the water level changed considerably towards the next month. The Landsat observation therefore likely measured different lake conditions than the satellite altimeter.

For 375 lakes with lower performance, the regression showed relatively low R^2 values with an average of 0.502. The most important reasons for these bad regressions were found to be winter ice or snow coverage, ~~small lake sizes,~~ cloud coverage, Landsat sensor issues and multiple individual lake compartments. Winter ice coverage influences both the altimetry accuracy and the accuracy in the GSW water classification (e.g. Lake Ulungur, Rybinsk Reservoir, Reindeer Lake and Lake Ilmen). The current methodology needs to be refined to include lakes that split into multiple lakes during extreme drying (e.g. Aral Sea). As the different compartments can have different water level dynamics, individual regressions would need to be assigned to each compartment to calculate volume fluctuations of each compartment individually. Further research on water losses in the Aral Sea using this technique could be very promising.

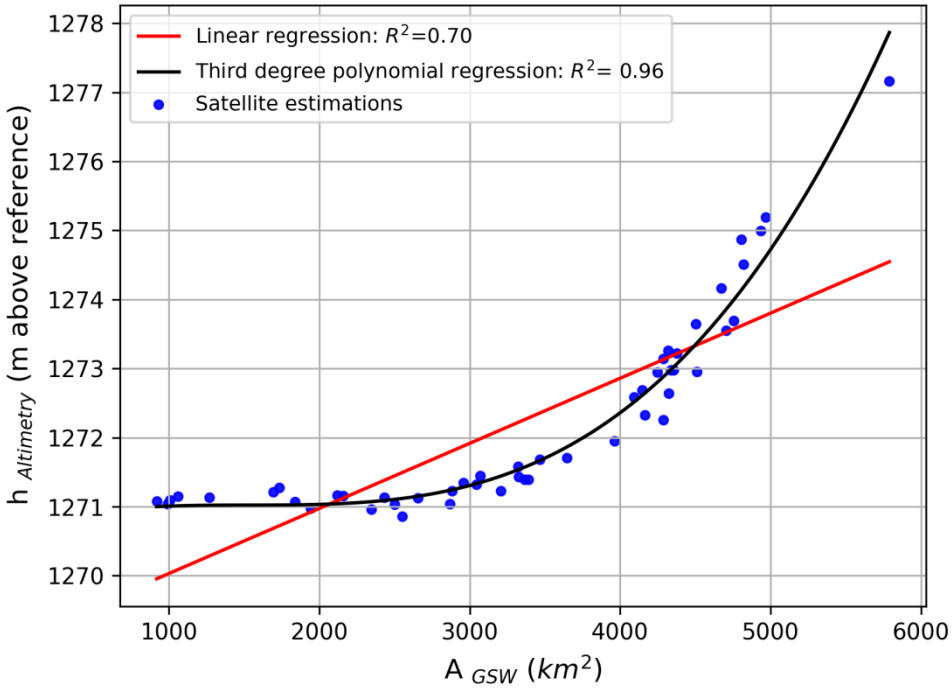

Figure 12 Relationship between A_{GSW} and $h_{Altimetry}$ for Lake Urmia. Only 3 out of the 135 lakes showed a clear non-linear relationship.

The calculated extrapolated volumes are more uncertain than the non-extrapolated ones, depending on whether the hypsometry relationship holds true or changes for the observed *h* or *A* value outside the regression range. For lakes formed in V-shaped river valleys with deep and straight slopes (e.g. Lake Mead), the hypsometry relationship is likely to hold for extremely low or high water levels. However, if the altimetry measurement period is short, the range of values captured by the regression line is likely to be small and the volume extrapolation using extreme level or area observations is expected to be inaccurate. This was observed for the Roseires Reservoir. However, including extrapolated volumes hardly changed the

overall validation results, because the amount of total extrapolated volumes compared to non-extrapolated volumes is very small.

6. Conclusions and perspectives

This study successfully combined the JRC Global Surface Water (GSW) dataset and the DAHITI satellite altimetry dataset to estimate lake and reservoir volume fluctuations over all continents. The GSW dataset records surface water over a 32-year period, containing 3066080 monthly images that cover 99.95 % of the landmass. The extensive size and high accuracy of this surface water dataset allowed for detailed volume variation estimations over a very long time period (1984-2015), without being constrained by complex and computationally intensive classification procedures.

Lake areas from the GSW dataset and water levels from the DAHITI altimetry dataset have been combined in a regression to explain the lake hypsometry of 1375 lakes globally. Nearly all lakes showed a linear regression. 587 of these lakes showed a highly accurate regression with $R^2 > 0.8$, with an average of 0.91. Lake volumes were calculated for all these lakes and for 421 other lakes with a nearly constant lake area. For 375 lakes, regressions were less accurate with an average R^2 of 0.502. Winter ice coverage, small lake size and no data in the GSW dataset were found to be most important reasons for low R^2 values.

For 98 100 lakes (587 variable area and 421 nearly constant area) volume variations were calculated by integrating the hypsometric relationships, using both area and water level observations separately. Decreases in water storage were found in Western U.S., where Lake Mead, Powell and the Great Salt Lake lost respectively 10 km^3, 6 km^3 and 16 km^3 of average volume between 1984-2000 and 2000-2015. According to our estimates, Lake Mead lost approximately 20 km^3 of water from 2000 to 2015. Using the USGS in situ measured storage volume of 31 km^3 in 2000, this is an almost 70 % reduction of water storage over last 15 years. Lake volume variation estimates have been validated for 18 lakes in the U.S., Spain, Australia and Africa using in situ lake volume time series. The estimated volume variations showed the method to be very accurate, expressed in an average Pearson correlation coefficient of 0.97, and a normalized RMSE of 7.42 %.

The low number of adequate Landsat lake area observations for some regions like Africa and Southwestern Europe still remains a limitation. Therefore, it would be highly beneficial for the purpose of this research to include surface water data from other satellites in the GSW dataset and to develop techniques to decrease the amount of no data in the current dataset. Future plans are to include Sentinel-1 and Sentinel-2 in the GSW dataset. The DAHITI database is continuously growing by analysing new water bodies, and newly available altimetry data will be processed to expand the volumetric dataset.

This lake and reservoir volume dataset will help to improve our current understanding of the behaviour of lakes and reservoirs, their representation in hydrological models and consequently the simulations of the river basin. This will moreover improve projections of the river basin under climate change or under different management scenarios and improve hydropower and open water evaporation estimations. The lake volume variations should be analysed to unravel the contributions of climate change, extreme climate phenomena (like El Niño and La Niña), human abstractions and dam

~~regulations on water storage changes. It is crucial to fully understand lake dynamics to improve future water resources projections in hydrological models and flood and drought forecasting systems.~~

This study constitutes a proof of concept paving the way for increasing the number of lakes and reservoirs analysed, which could potentially be included as an a priori water storage dataset for the Surface Water and Ocean Topography (SWOT) hydrology and oceanography satellite mission. Launched in 2020, this mission will combine water body contours and accurate water level estimations to estimate storage changes in lakes and reservoirs with an average accuracy of 20 cm (Biancamaria et al., 2016; Crétaux et al., 2015). The SWOT satellite will be unique due to its accuracy and capabilities on smaller water bodies with a size of at least 250 x 250 m.

Data availability. Underlying research data are not publicly accessible. Lakes and reservoir volumes may become publicly available in a later stage through the DAHITI web service (http://dahiti.dgfi.tum.de/en/). The access to remote sensing data used in this study is explained in Sect. 2.

Appendix 1

Constant area lakes (Lc) overview

Lake/ Reservoir name	Latitude	Longitude	min area (km^2)	max area (km^2)	CV area	min water level (m)	max water level (m)	R2 regression	Average volume change between 2000-2008 and 2008-2015 (km^3)
Albert	1.63	30.91	5354.80	5412.16	0.003	620.71	622.55	0.01	-3.49
Argentino	-50.24	-72.84	1546.95	1555.79	0.004	177.04	180.78	0.01	0.40
Athabasca	59.19	-109.28	7528.69	7723.01	0.005	208.71	211.31	0.53	-0.59
Baikal	53.36	107.57	31572.61	31963.98	0.003	455.00	455.95	0.00	2.54
Baker	64.16	-95.28	1697.53	1723.77	0.004	0.62	2.14	0.45	0.44
Balaton	46.86	17.75	573.48	582.15	0.003	103.98	105.24	0.03	-
Buenos Aires	-46.55	-71.97	1832.01	1862.79	0.003	205.25	207.13	0.23	0.13
Chiemsee	47.88	12.45	74.89	76.50	0.005	517.86	519.55	0.27	-0.01
Constance	47.61	9.42	466.60	469.81	0.002	394.09	396.01	0.22	0.12
Dore	54.77	-107.31	621.17	632.80	0.004	458.79	459.94	0.49	0.28
Edward	-0.36	29.59	2209.06	2235.13	0.003	913.98	915.54	0.37	0.52
Erie	42.14	-81.29	25488.04	25789.63	0.003	173.55	174.87	0.00	2.36
Flathead	47.88	-114.14	480.89	494.76	0.006	878.96	882.12	0.40	-0.13
Great Bear	66.00	-120.97	30266.01	30555.78	0.003	156.95	157.75	0.17	4.49
Huron	45.01	-82.29	58972.33	59664.21	0.003	175.32	176.97	0.10	8.16
Issyk-Kul	42.44	77.27	6165.81	6220.68	0.002	1605.55	1606.32	0.04	0.16
Keller	63.93	-121.58	389.56	393.02	0.002	239.69	240.77	0.07	0.06
Khuvsgul	51.06	100.47	2758.95	2788.74	0.002	1646.49	1647.39	0.03	0.56
Kivu	-2.04	29.10	2368.70	2395.02	0.003	1460.74	1462.34	0.00	0.56
Kremenchuk	49.30	32.68	1828.27	1914.02	0.006	76.70	81.57	0.32	0.35
Ladoga	60.84	31.47	17330.63	17601.68	0.003	2.27	5.11	0.03	8.10
Llanquihue	-41.14	-72.82	855.85	864.19	0.002	50.00	51.00	0.00	-0.08
Malawi	-12.02	34.53	29195.33	29550.33	0.003	472.15	475.22	0.03	-4.18
Michigan	44.02	-86.76	57283.26	57856.91	0.002	175.25	176.91	0.00	7.59
Mweru	-9.02	28.72	4963.59	5104.84	0.006	923.20	926.72	0.01	2.24
Nicaragua	11.53	-85.41	7749.76	7815.10	0.003	30.05	32.56	0.02	1.22
Nipigon	49.81	-88.52	4462.91	4515.99	0.003	259.49	260.91	0.00	1.24
Novosibirsk	54.54	82.37	976.27	998.96	0.005	111.69	114.47	0.00	-0.02
Ontario	43.64	-77.81	18529.57	18741.92	0.003	73.97	75.37	0.04	0.37
Peipus	58.54	27.55	3465.82	3556.71	0.005	28.78	31.13	0.18	0.62
Porisvatn	64.27	-18.86	84.49	85.26	0.003	570.71	580.61	0.60	-0.06

Ranco	-40.24	-72.40	424.58	429.46	0.003	63.10	65.96	0.00	0.00
Saint Jean	48.59	-72.04	1063.55	1086.20	0.004	97.74	101.87	0.07	0.06
Shala	7.47	38.51	299.65	308.01	0.006	1553.45	1555.58	0.38	-0.14
Superior	47.55	-87.78	81320.65	82151.16	0.003	182.32	183.43	0.02	5.31
Tanganyika	-6.22	29.89	32400.06	32685.75	0.003	768.43	770.94	0.03	14.04
Uvs	50.32	92.75	3486.72	3628.63	0.008	761.81	763.25	0.57	-1.26
Vanern	58.90	13.27	5300.96	5414.91	0.005	44.22	45.33	0.12	0.95
Victoria	-1.12	32.90	66123.35	66765.69	0.004	1133.55	1135.95	0.07	11.55
Wollaston	58.23	-103.29	2192.42	2227.67	0.004	395.51	396.90	0.03	0.01
Yellowstone	44.43	-110.37	338.88	343.35	0.003	2357.03	2358.79	0.45	0.10
Zhari Namco	30.92	85.62	977.33	1007.46	0.007	4610.14	4613.18	0.56	0.97

Variable area lakes (LvG) overview

Lake/reservoir name	Latitude	Longitude	min area (km^2)	max area (km^2)	CV area	min water level (m)	max water level (m)	R2 regression	Average volume change between 1984-2000 and 2000-2016 (km^3)
Alcantara	39.77	-6.67	43.22	63.72	0.098	187.83	216.33	0.88	0.43
Almanor	40.25	-121.14	87.07	100.89	0.028	1367.71	1373.24	0.85	0.03
Alvaro Obregon	27.96	-109.86	34.71	177.09	0.394	64.51	93.03	0.91	-0.29
Angostura	16.12	-92.64	265.26	562.21	0.143	496.84	527.92	0.98	-1.71
Argyle	-16.34	128.75	346.54	1187.54	0.195	88.66	95.83	0.89	3.30
Assad	36.00	38.26	518.94	643.55	0.044	297.60	304.36	0.85	0.52
Bagre	11.56	-0.68	0.00	195.02	0.555	227.12	236.06	0.98	0.44
Balbina	-1.44	-59.89	23.36	2421.59	0.315	42.12	49.09	0.92	5.51
Barragem do Caia	39.03	-7.19	5.54	15.72	0.197	222.06	233.22	0.97	0.01
Berryessa	38.58	-122.22	45.30	72.77	0.101	120.67	134.76	0.95	0.28
Boston	41.97	87.06	901.79	1063.23	0.052	1045.34	1049.88	0.98	0.31
Brahmamsagar	14.78	78.89	0.09	21.30	0.930	186.79	209.36	0.99	0.13
Bratsk	55.87	102.34	2908.56	3126.58	0.019	395.21	402.24	0.88	-
Cahora Bassa	-15.68	31.67	1629.92	2481.94	0.128	318.20	327.01	0.94	19.38
Chapala	20.24	-103.02	717.29	1102.63	0.107	1517.52	1522.95	0.82	-0.08
Chiquita	-30.54	-62.66	2866.43	6763.70	0.204	67.41	72.51	0.84	-0.48
Encoro de Salas	41.92	-7.93	1.06	3.75	0.191	815.95	828.93	0.95	0.01
Eucumbene	-36.08	148.70	53.47	131.58	0.210	1117.82	1155.38	0.97	-1.35
Great Salt Lake	41.18	-112.53	3228.40	6205.50	0.182	1278.83	1283.74	0.93	-15.72
Guri	7.40	-62.86	2914.13	3507.38	0.076	243.73	271.17	0.99	-7.26

Houston	29.98	-95.14	31.19	38.24	0.031	11.34	13.70	0.87	0.00
Hubbard Creek	32.79	-99.01	15.28	58.58	0.281	351.42	360.75	0.98	-0.14
Hulun	48.95	117.40	1782.96	2122.60	0.050	540.45	544.01	0.97	-3.01
Kainji	10.32	4.56	724.06	1134.86	0.075	128.60	139.71	0.93	-0.48
Kajaki	32.33	65.19	23.08	38.44	0.088	998.19	1021.17	0.88	-0.03
Kapchagay	43.82	77.61	1119.35	1242.98	0.021	475.34	479.41	0.94	0.17
Karakaya Baraji	38.53	38.47	21.41	236.14	0.141	673.61	692.12	0.97	0.81
Kariba	-16.99	28.04	4571.10	5323.91	0.041	475.54	487.09	0.96	15.28
Khyargas Nuur	49.18	93.32	1364.23	1397.40	0.008	1027.99	1032.76	0.97	1.49
Manitoba	50.98	-98.70	4700.32	5022.90	0.012	246.51	248.63	0.82	0.47
Manso	-14.95	-55.66	0.24	339.87	0.847	283.03	287.27	0.83	4.72
Massinger	-23.89	32.04	16.25	128.93	0.342	100.50	123.66	0.93	1.10
Barragen Mead	36.19	-114.41	327.92	580.50	0.181	328.69	353.61	0.98	-10.75
Nasser	22.88	32.33	3156.39	5770.06	0.128	166.85	181.08	0.92	-1.79
Netzahualcoyotl	17.14	-93.63	228.21	281.65	0.053	151.88	177.34	0.94	-1.12
O. H. Ivie	31.55	-99.72	0.10	70.45	0.642	458.64	469.13	0.97	-0.15
Powell	37.24	-110.96	311.38	555.09	0.169	1086.86	1126.50	0.99	-6.35
Puente Nuevo	38.13	-4.97	3.44	17.87	0.401	437.24	444.78	0.91	0.10
Qarun	29.47	30.63	226.46	255.33	0.032	-42.59	-41.40	0.86	0.12
Qinghai	36.89	100.20	4217.58	4369.47	0.012	3193.29	3194.35	0.83	-0.36
Richland	31.99	-96.26	1.32	174.31	0.372	93.08	96.64	0.92	0.27
Chambers Roseires	11.60	34.46	88.65	578.54	0.436	471.70	487.74	0.84	2.06
Rukwa	-7.96	32.21	5388.63	6057.51	0.039	799.90	804.28	0.88	-13.01
Sam Rayburn	31.22	-94.24	290.73	429.91	0.067	46.35	53.02	0.88	0.00
Sarygamysh	41.93	57.41	3086.11	3967.24	0.065	0.53	8.49	0.99	20.50
Serena	38.89	-5.18	3.18	125.32	0.386	330.93	349.84	0.96	1.69
Siling Co	31.80	88.99	2324.93	2401.16	0.01	4537.72	4543.97	0.89	17.56
Sobradinho	-9.67	-41.62	1501.04	3446.70	0.216	384.92	394.58	0.86	-2.20
Tengiz	50.44	69.08	861.36	1632.89	0.168	304.32	306.60	0.95	-1.25
Tharthar	34.01	43.26	1593.83	2286.33	0.119	42.76	63.60	0.94	-16.29
Titicaca	-15.90	-69.33	7513.44	8361.62	0.023	3809.10	3811.66	0.81	-2.60
Toktogul	41.79	72.90	195.07	289.14	0.117	856.13	898.94	0.91	-0.73
Toledo Bend	31.47	-93.72	472.87	630.83	0.056	48.86	52.65	0.81	0.01
Volta	7.44	-0.18	4645.90	6885.92	0.124	74.54	84.85	0.96	-14.51
Walker	38.68	-118.71	111.70	154.99	0.081	1191.20	1205.93	0.98	-0.96
Williston	56.08	-123.66	1495.12	1715.51	0.031	656.92	671.72	0.84	2.72
Winnipegosis	52.55	-100.15	5027.12	5257.38	0.008	252.43	254.72	0.87	2.78
Yesa	42.61	-1.11	11.50	17.42	0.086	459.12	486.80	0.86	0.02

Less performant variable area lakes (LvP) overview

Lake/reservoir name	Latitude	Longitude	min area (km^2)	max area (km^2)	CV area	min water level (m)	max water level (m)	R2 regression
Altmuhl	49.13	10.72	3.28	3.44	0.012	414.00	416.01	0.19
Aydar	40.87	66.91	1661.19	3228.23	0.174	244.61	248.04	0.71
Bardwell	32.28	-96.66	10.72	14.48	0.046	127.03	131.91	0.55
Beysehir	37.78	31.51	611.43	669.54	0.020	1120.43	1124.22	0.73
Caddabassa	8.87	39.87	30.15	48.89	0.141	560.51	563.13	0.11
Caddo	32.71	-94.02	40.75	63.30	0.125	50.59	52.87	0.44
Cedar	53.34	-100.17	2358.60	2709.49	0.025	252.59	256.56	0.45
Chad	13.04	14.49	1241.46	1459.73	0.044	279.96	282.13	0.30
Chamo	5.85	37.55	292.56	330.97	0.030	1105.26	1108.24	0.66
Churumuco	18.56	-101.86	156.26	309.69	0.157	137.28	161.38	0.51
Claire	58.59	-112.09	1231.20	1416.09	0.036	209.60	210.73	0.21
Danau Tang	0.63	112.47	2.81	6.50	0.170	17.77	24.78	0.62
Eagle	40.65	-120.73	51.08	102.63	0.093	1551.70	1556.77	0.75
Fairfield	31.79	-96.06	6.12	8.03	0.059	92.84	95.17	0.26
Hainer	51.17	12.46	0.00	3.70	0.586	123.52	127.82	0.00
Ilmen	58.25	31.38	941.97	1306.72	0.112	15.84	21.45	0.62
Kusai	35.73	92.87	263.91	332.97	0.087	4475.46	4484.40	0.13
Kuybyshev	54.60	49.17	4529.53	4839.51	0.012	47.73	53.17	0.61
Lesser Slave	55.44	-115.40	1120.94	1182.22	0.009	576.09	578.14	0.60
Mosul Dam	36.74	42.75	12.90	331.67	0.224	303.70	329.06	0.73
Musters	-45.40	-69.20	422.71	465.35	0.025	268.54	271.00	0.78
Nam Co	30.74	90.61	1948.79	2024.41	0.011	4721.94	4724.39	0.55
Poopo	-18.76	-67.09	10.62	3104.92	0.583	3685.50	3686.24	0.21
Reindeer	57.28	-102.38	5201.41	5422.67	0.010	335.58	337.42	0.67
Resia	46.80	10.53	5.77	6.12	0.015	1476.00	1496.18	0.76
Rybinsk	58.52	38.28	3590.26	3778.11	0.012	97.96	101.16	0.53
Tai Hu	31.20	120.23	2216.78	2359.42	0.016	1.36	2.67	0.00
Tana	11.99	37.31	2986.63	3107.77	0.008	1784.94	1788.29	0.74
Tangra Yumco	31.06	86.60	831.89	860.39	0.008	4531.35	4536.80	0.56
Tawakoni	32.89	-96.00	106.85	150.45	0.070	131.01	134.08	0.76
Thulsfelder	52.93	7.93	0.42	1.18	0.162	21.61	23.03	0.63
Tsimlyansk	47.96	42.79	1988.14	2366.59	0.031	31.70	36.38	0.80
Turkana	3.51	36.20	7033.64	7501.42	0.015	360.37	365.18	0.71
Ulungur	47.25	87.29	852.58	887.48	0.009	482.36	484.04	0.24

Urmia	37.64	45.50	917.87	5790.55	0.372	1270.11	1278.01	0.70
Zama	58.79	-119.03	65.19	288.52	0.443	325.88	328.81	0.28
Zaysan	48.01	83.89	2829.26	3253.41	0.032	388.60	394.87	0.56

Author contribution. T. B. developed the methodology, the scripts and was the main writer of the paper. A.R. helped writing the introduction section and gave comprehensive scientific support over the whole period. E.G. considerably supported in designing the methodology and in coding the scripts. C.S. provided DAHITI altimetry data, additionally processed water bodies on demand and moreover wrote the altimetry section. J.F.P. and A.C. contributed in the Google Earth Engine usage and wrote the GSW section. All authors actively contributed to the feedback process after the first draft.

Competing interests. The authors declare that they have no conflict of interest.

Acknowledgements. We would like to thank the Google Earth Engine team, and especially Matthew Hancher and Noel Gorelick, for support in developing the Earth Engine scripts. We would also like to express our gratitude to Guido Lemoine (Joint Research Centre) for his technical support in Earth Engine and Steven de Jong (Utrecht University) for his feedback on the first report.

References

Avisse, N., Tilmant, A., Müller, M. F. and Zhang, H.: Monitoring small reservoirs storage from satellite remote sensing in inaccessible areas, Hydrol. Earth Syst. Sci., 21(12), 6445–6459, doi:10.5194/hess-21-6445-2017, 2017.

Balmer, M. and Downing, J.: Carbon dioxide concentrations in eutrophic lakes: undersaturation implies atmospheric uptake, Inl. Waters, 1(2), 125–132, doi:10.5268/IW-1.2.366, 2011.

Barnett, T. P. and Pierce, D. W.: When will Lake Mead go dry?, Water Resour. Res., 44(3), doi:10.1029/2007WR006704, 2008.

Benenati, E. P., Shannon, J. P., Blinn, D. W., Wilson, K. P. and Hueftle, S. J.: Reservoir-river linkages: Lake Powell and the Colorado River, Arizona, J. North Am. Benthol. Soc., 19(4), 742–755, doi:10.2307/1468131, 2000.

Berg, H., Michélsen, P., Troell, M., Folke, C. and Kautsky, N.: Managing aquaculture for sustainability in tropical Lake Kariba, Zimbabwe, Ecol. Econ., 18(2), 141–159, doi:10.1016/0921-8009(96)00018-3, 1996.

Biancamaria, S., Lettenmaier, D. P. and Pavelsky, T. M.: The SWOT Mission and Its Capabilities for Land Hydrology, Surv. Geophys., 37(2), 307–337, doi:10.1007/s10712-015-9346-y, 2016.

Biemans, H., Haddeland, I., Kabat, P., Ludwig, F., Hutjes, R. W. A., Heinke, J., von Bloh, W. and Gerten, D.: Impact of reservoirs on river discharge and irrigation water supply during the 20th century, Water Resour. Res., 47(3), doi:10.1029/2009WR008929, 2011.

Birkett, C. M.: The contribution of TOPEX/POSEIDON to the global monitoring of climatically sensitive lakes, J. Geophys. Res., 100204(15), 179–25, doi:10.1029/95JC02125, 1995.

Boergens, E., Dettmering, D., Schwatke, C. and Seitz, F.: Treating the hooking effect in satellite altimetry data: A case study along the mekong river and its tributaries, Remote Sens., 8(2), doi:10.3390/rs8020091, 2016.

Bosch, W., Dettmering, D. and Schwatke, C.: Multi-mission cross-calibration of satellite altimeters: Constructing a long-term data record for global and regional sea level change studies, Remote Sens., 6(3), 2255–2281, doi:10.3390/rs6032255, 2014.

Chao, B. F., Wu, Y. H. and Li, Y. S.: Impact of artificial reservoir water impoundment on global sea level., Science, 320(5873), 212–214, doi:10.1126/science.1154580, 2008.

Cole, J. J., Prairie, Y. T., Caraco, N. F., McDowell, W. H., Tranvik, L. J., Striegl, R. G., Duarte, C. M., Kortelainen, P., Downing, J. A., Middelburg, J. J. and Melack, J.: Plumbing the global carbon cycle: Integrating inland waters into the terrestrial carbon budget, Ecosystems, 10(1), 171–184, doi:10.1007/s10021-006-9013-8, 2007.

Cook, E. R., Seager, R., Cane, M. A. and Stahle, D. W.: North American drought: Reconstructions, causes, and consequences, Earth-Science Rev., 81(1–2), 93–134, doi:10.1016/j.earscirev.2006.12.002, 2007.

Crétaux, J.-F., Biancamaria, S., Arsen, A., Bergé Nguyen, M. and Becker, M.: Global surveys of reservoirs and lakes from satellites and regional application to the Syrdarya river basin, Environ. Res. Lett., 10(1), 15002, doi:10.1088/1748-9326/10/1/015002, 2015.

Crétaux, J.-F., Abarca-del-Río, R., Bergé-Nguyen, M., Arsen, A., Drolon, V., Clos, G. and Maisongrande, P.: Lake Volume Monitoring from Space, Surv. Geophys., 37(2), 269–305, doi:10.1007/s10712-016-9362-6, 2016.

Downing, J. A., Prairie, Y. T., Cole, J. J., Duarte, C. M., Tranvik, L. J., Striegl, R. G., McDowell, W. H., Kortelainen, P., Caraco, N. F., Melack, J. M. and Middelburg, J. J.: The global abundance and size distribution of lakes, ponds, and impoundments, Limnol. Oceanogr., 51(5), 2388–2397, doi:10.4319/lo.2006.51.5.2388, 2006.

Duan, Z. and Bastiaanssen, W. G. M.: Estimating water volume variations in lakes and reservoirs from four operational satellite altimetry databases and satellite imagery data, Remote Sens. Environ., 134, 403–416, doi:10.1016/j.rse.2013.03.010, 2013.

Frappart, F., Calmant, S., Cauhopé, M., Seyler, F. and Cazenave, A.: Preliminary results of ENVISAT RA-2-derived water levels validation over the Amazon basin, Remote Sens. Environ., 100(2), 252–264, doi:10.1016/j.rse.2005.10.027, 2006a.

Frappart, F., Do Minh, K., L'Hermitte, J., Cazenave, A., Ramillien, G., Le Toan, T. and Mognard-Campbell, N.: Water volume change in the lower Mekong from satellite altimetry and imagery data, Geophys. J. Int., 167(2), 570–584, doi:10.1111/j.1365-246X.2006.03184.x, 2006b.

Frey, K. E. and Smith, L. C.: Amplified carbon release from vast West Siberian peatlands by 2100, Geophys. Res. Lett., 32(9), 1–4, doi:10.1029/2004GL022025, 2005.

Fu, L. L. and Cazenave, A.: Satellite altimetry and earth sciences: a handbook of techniques and applications, Academic Press., 2001.

Gao, H., Birkett, C. and Lettenmaier, D. P.: Global monitoring of large reservoir storage from satellite remote sensing, Water Resour. Res., 48(9), 1–12, doi:10.1029/2012WR012063, 2012.

Gorelick, N., Hancher, M., Dixon, M., Ilyushchenko, S., Thau, D. and Moore, R.: Google Earth Engine: Planetary-scale geospatial analysis for everyone, Remote Sens. Environ., doi:10.1016/j.rse.2017.06.031, 2017.

Haddeland, I., Heinke, J., Biemans, H., Eisner, S., Flörke, M., Hanasaki, N., Konzmann, M., Ludwig, F., Masaki, Y., Schewe, J., Stacke, T., Tessler, Z. D., Wada, Y. and Wisser, D.: Global water resources affected by human interventions and climate change, Proc. Natl. Acad. Sci., 111(9), 3251–3256, doi:10.1073/pnas.1222475110, 2014.

Hanasaki, N., Kanae, S. and Oki, T.: A reservoir operation scheme for global river routing models, J. Hydrol., 327(1–2), 22–41, doi:10.1016/j.jhydrol.2005.11.011, 2006.

Holdren, G. C. and Turner, K.: Characteristics of Lake Mead, Arizona-Nevada, Lake Reserv. Manag., 26(4), 230–239, doi:10.1080/07438141.2010.540699, 2010.

Hwang, C., Guo, J., Deng, X., Hsu, H. Y. and Liu, Y.: Coastal gravity anomalies from retracked Geosat/GM altimetry: Improvement, limitation and the role of airborne gravity data, J. Geod., 80(4), 204–216, doi:10.1007/s00190-006-0052-x, 2006.

Kouraev, A. V., Zakharova, E. A., Samain, O., Mognard, N. M. and Cazenave, A.: Ob' river discharge from TOPEX/Poseidon satellite altimetry (1992-2002), Remote Sens. Environ., 93(1–2), 238–245, doi:10.1016/j.rse.2004.07.007, 2004.

LakeNet: Lake profile: Kariba, [online] Available from: http://www.worldlakes.org/lakedetails.asp?lakeid=8360 (Accessed 2 January 2018), 2003.

Lehner, B. and Döll, P.: Development and validation of a global database of lakes, reservoirs and wetlands, J. Hydrol., 296(1), 1–22, doi:10.1016/j.jhydrol.2004.03.028, 2004.

Liu, Q.: Interlinking climate change with water-energy-food nexus and related ecosystem processes in California case studies, Ecol. Process., 5(1), doi:10.1186/s13717-016-0058-0, 2016.

Meybeck, M.: Global distribution of lakes, in Physics and Chemistry of Lakes, pp. 1–35, Spinger, Berlin, Germany., 1995.

Micklin, P.: The future Aral Sea: hope and despair, Environ. Earth Sci., 75(9), 844, doi:10.1007/s12665-016-5614-5, 2016.

Muala, E., Mohamed, Y. A., Duan, Z. and van der Zaag, P.: Estimation of reservoir discharges from Lake Nasser and Roseires Reservoir in the Nile Basin using satellite altimetry and imagery data, Remote Sens., 6(8), 7522–7545, doi:10.3390/rs6087522, 2014.

Pekel, J.-F., Cottam, A., Gorelick, N. and Belward, A. S.: High-resolution mapping of global surface water and its long-term changes, Nature, 1–19, doi:10.1038/nature20584, 2016.

Ran, L. and Lu, X. X.: Delineation of reservoirs using remote sensing and their storage estimate: An example of the Yellow River basin, China, Hydrol. Process., 26(8), 1215–1229, doi:10.1002/hyp.8224, 2012.

Richey, J. E., Melack, J. M., Aufdenkampe, A. K., Ballester, V. M. and Hess, L. L.: Outgassing from Amazonian rivers and wetlands as a large tropical source of atmospheric CO2., Nature, 416(6881), 617–620, doi:10.1038/416617a, 2002.

Schwatke, C., Dettmering, D., Bosch, W. and Seitz, F.: DAHITI - An innovative approach for estimating water level time series over inland waters using multi-mission satellite altimetry, Hydrol. Earth Syst. Sci., 19(10), 4345–4364, doi:10.5194/hess-19-4345-2015, 2015a.

Schwatke, C., Dettmering, D., Börgens, E. and Bosch, W.: Potential of SARAL/AltiKa for Inland Water Applications, Mar. Geod., 38, 626–643, doi:10.1080/01490419.2015.1008710, 2015b.

Smith, L. C. and Pavelsky, T. M.: Remote sensing of volumetric storage changes in lakes, Earth Surf. Process. Landforms, 34(10), 1353–1358, doi:10.1002/esp.1822, 2009.

Tong, X., Pan, H., Xie, H., Xu, X., Li, F., Chen, L., Luo, X., Liu, S., Chen, P. and Jin, Y.: Estimating water volume variations in Lake Victoria over the past 22years using multi-mission altimetry and remotely sensed images, Remote Sens. Environ., 187, 400–413, doi:10.1016/j.rse.2016.10.012, 2016.

Tourian, M. J., Schwatke, C. and Sneeuw, N.: River discharge estimation at daily resolution from satellite altimetry over an entire river basin, J. Hydrol., 546, 230–247, doi:10.1016/j.jhydrol.2017.01.009, 2017.

Verpoorter, C., Kutser, T., Seekell, D. A. and Tranvik, L. J.: A global inventory of lakes based on high-resolution satellite imagery, Geophys. Res. Lett., 41(18), 6396–6402, doi:10.1002/2014GL060641, 2014.

Villadsen, H., Andersen, O. B., Stenseng, L., Nielsen, K. and Knudsen, P.: CryoSat-2 altimetry for river level monitoring - Evaluation in the Ganges-Brahmaputra River basin, Remote Sens. Environ., 168, 80–89, doi:10.1016/j.rse.2015.05.025, 2015.

Wulder, M. A., White, J. C., Loveland, T. R., Woodcock, C. E., Belward, A. S., Cohen, W. B., Fosnight, E. A., Shaw, J., Masek, J. G. and Roy, D. P.: The global Landsat archive: Status, consolidation, and direction, Remote Sens. Environ., 185, 271–283, doi:10.1016/j.rse.2015.11.032, 2016.

Zajac, Z., Revilla-Romero, B., Salamon, P., Burek, P., Hirpa, F. and Beck, H.: The impact of lake and reservoir parameterization on global streamflow simulation, J. Hydrol., 548, 552–568, doi:10.1016/j.jhydrol.2017.03.022, 2017.

Zakharova, E. A., Kouraev, A. V., Cazenave, A. and Seyler, F.: Amazon River discharge estimated from TOPEX/Poseidon altimetry, Comptes Rendus Geosci., 338(3), 188–196, doi:10.1016/j.crte.2005.10.003, 2006.

Zhang, G., Xie, H., Kang, S., Yi, D. and Ackley, S. F.: Monitoring lake level changes on the Tibetan Plateau using ICESat altimetry data (2003-2009), Remote Sens. Environ., 115(7), 1733–1742, doi:10.1016/j.rse.2011.03.005, 2011.

Zhang, J., Xu, K., Yang, Y., Qi, L., Hayashi, S. and Watanabe, M.: Measuring water storage fluctuations in Lake Dongting, China, by Topex/Poseidon satellite altimetry, Environ. Monit. Assess., 115(1–3), 23–37, doi:10.1007/s10661-006-5233-9, 2006.

Zhou, Y., Jin, S., Tenzer, R. and Feng, J.: Water storage variations in the Poyang Lake Basin estimated from GRACE and satellite altimetry, Geod. Geodyn., 7(2), 108–116, doi:10.1016/j.geog.2016.04.003, 2016.

Table 1 Overview of the validation results, excluding and including extrapolated volumes.

		Extrapolated volumes excluded			*Extrapolated volumes included*		
Lake/reservoir name:		**Pearsons *r***	**RMSE (km^3)**	**NRMSE (%)**	**Pearsons *r***	**RMSE (km^3)**	**NRMSE (%)**
Alcantara	GSW dataset:	0.941	0.229	12.750	0.941	0.229	12.750
	Altimetry:	0.986	0.151	8.427	0.987	0.153	8.265
Almanor	GSW dataset:	0.902	0.060	11.340	0.908	0.071	11.122
	Altimetry:	0.990	0.019	3.676	0.989	0.020	3.874
Argyle	GSW dataset:	0.954	0.471	7.924	0.954	0.471	7.924
	Altimetry:	0.995	0.147	2.474	0.995	0.147	2.474
Berryessa	GSW dataset:	0.961	0.063	7.448	0.989	0.076	5.311
	Altimetry:	0.978	0.043	5.575	0.978	0.043	5.575
Encoro de Salas	GSW dataset:	0.966	0.004	8.358	0.966	0.004	7.455
	Altimetry:	0.985	0.002	7.323	0.992	0.003	6.145
Eucumbene	GSW dataset:	0.933	0.114	11.802	0.933	0.114	11.802
	Altimetry:	0.964	0.084	8.419	0.964	0.084	8.419
Houston	GSW dataset:	0.904	0.008	10.235	0.904	0.008	10.235
	Altimetry:	0.938	0.005	5.666	0.938	0.005	5.436
Hubbard Creek	GSW dataset:	0.985	0.017	5.173	0.988	0.018	5.372
	Altimetry:	0.998	0.006	1.924	0.999	0.007	2.118
Mead	GSW dataset:	0.985	0.449	4.685	0.997	1.045	5.434
	Altimetry:	0.998	0.179	1.865	0.998	0.179	1.865
O. H. Ivie	GSW dataset:	0.985	0.019	4.924	0.993	0.030	4.950
	Altimetry:	0.999	0.006	1.784	0.999	0.006	1.784
Powell	GSW dataset:	0.993	0.913	4.947	0.994	0.923	4.524
	Altimetry:	0.997	0.552	3.074	0.998	0.554	2.964
Puente Nuevo	GSW dataset:	0.961	0.011	9.182	0.991	0.013	5.329
	Altimetry:	0.993	0.006	4.972	0.994	0.006	4.954
Richland Chambers	GSW dataset:	0.954	0.046	9.161	0.954	0.046	9.161
	Altimetry:	0.989	0.023	4.224	0.990	0.022	4.196
Roseires	GSW dataset:	0.805	0.295	18.872	0.971	2.434	41.455
	Altimetry:	0.925	0.214	12.443	0.962	0.214	11.473
Serena	GSW dataset:	0.989	0.092	4.907	0.989	0.122	3.767
	Altimetry:	0.990	0.077	4.294	0.990	0.077	4.294
Toledo Bend	GSW dataset:	0.765	0.351	14.376	0.777	0.345	14.135
	Altimetry:	0.988	0.122	5.015	0.988	0.121	4.974
Walker	GSW dataset:	0.936	0.071	10.798	0.971	0.072	8.180
	Altimetry:	0.988	0.032	4.882	0.990	0.041	4.499

Yesa reservoir	GSW dataset:	0.919	0.030	11.863	0.960	0.029	8.071
	Altimetry:	0.983	0.015	6.228	0.979	0.024	6.971
Average		**0.959**	**0.137**	**7.250**	**0.970**	**0.215**	**7.424**